



National Library of Canada

Cataloguing Branch
Canadian Theses Division

Ottawa, Canada
K1A 0N4

Bibliothèque nationale du Canada

Direction du catalogage
Division des thèses canadiennes

NOTICE

The quality of this microfiche is heavily dependent upon the quality of the original thesis submitted for microfilming. Every effort has been made to ensure the highest quality of reproduction possible.

If pages are missing, contact the university which granted the degree.

Some pages may have indistinct print especially if the original pages were typed with a poor typewriter ribbon or if the university sent us a poor photocopy.

Previously copyrighted materials (journal articles, published tests, etc.) are not filmed.

Reproduction in full or in part of this film is governed by the Canadian Copyright Act, R.S.C. 1970, c. C-30. Please read the authorization forms which accompany this thesis.

**THIS DISSERTATION
HAS BEEN MICROFILMED
EXACTLY AS RECEIVED**

AVIS

La qualité de cette microfiche dépend grandement de la qualité de la thèse soumise au microfilmage. Nous avons tout fait pour assurer une qualité supérieure de reproduction.

S'il manque des pages, veuillez communiquer avec l'université qui a conféré le grade.

La qualité d'impression de certaines pages peut laisser à désirer, surtout si les pages originales ont été dactylographiées à l'aide d'un ruban usé ou si l'université nous a fait parvenir une photocopie de mauvaise qualité.

Les documents qui font déjà l'objet d'un droit d'auteur (articles de revue, examens publiés, etc.) ne sont pas microfilmés.

La reproduction, même partielle, de ce microfilm est soumise à la Loi canadienne sur le droit d'auteur, SRC 1970, c. C-30. Veuillez prendre connaissance des formules d'autorisation qui accompagnent cette thèse.

**LA THÈSE A ÉTÉ
MICROFILMÉE TELLE QUE
NOUS L'AVONS REÇUE**

THE PHYSICAL METALLURGY OF THE WELD HEAT-AFFECTED-ZONE IN STEELS

Brian A. Graville

A Major Technical Report
In The
Faculty of Engineering

Presented in Partial Fulfilment of the Requirements for the
Degree of Master of Engineering at
Concordia University
Montreal, Canada

June 1978

© Brian A. Graville, 1978

ABSTRACT

THE PHYSICAL METALLURGY OF THE WELD HEAT-AFFECTED-ZONE IN STEELS

Brian A. Graville

The metallurgy of the heat-affected-zone (HAZ) is reviewed with particular emphasis on modern high strength low alloy (microalloyed) steels. The development of modern steels is briefly reviewed and the role of microalloy additions, such as niobium, is highlighted. Thermal conditions in the HAZ are described in terms of classical heat flow theory and the effect on grain growth is reviewed. Precipitation phenomena are discussed. In most cases cooling rates are too rapid for extensive precipitation, although it can occur with high energy welding processes or after a post-weld heat treatment. Precipitation hardening can lead to a decrease in toughness, but the removal of nitrogen from solid solution can have a beneficial effect.

Recent studies of the fracture toughness of the HAZ are reviewed and a discussion is included of areas that require study in order to improve the understanding of the physical metallurgy of the HAZ of steels.

9

ACKNOWLEDGEMENTS

The author wishes to record his gratitude to Prof. H. McQueen for much help and guidance during his studies and during the preparation of this report. Other members of staff and colleagues have been of assistance and their contributions are greatly appreciated.

TABLE OF CONTENTS

	<u>Page</u>
ABSTRACT	iii
ACKNOWLEDGEMENTS	v
TABLE OF CONTENTS	vi
LIST OF FIGURES	vii
1. INTRODUCTION	1
2. DEVELOPMENT OF STEELS	2
2.1. Steels and Weldability	2
2.2. Microalloy Steels	5
3. THERMAL CONDITIONS IN THE HEAT-AFFECTED-ZONE	16
3.1. Point Source Theory	17
3.2. Grain Coarsening	26
4. HARDNESS OF THE HEAT-AFFECTED-ZONE	31
5. MICROALLOY ELEMENTS IN THE HAZ	36
6. REVIEW OF TOUGHNESS STUDIES ON THE HAZ OF MICROALLOY STEELS	43
7. SUMMARY AND CONCLUSIONS	66

LIST OF FIGURES

- Figure 1 : Increase in Yield Stress, Δy Plotted Against the Austenitizing Temperature of the Niobium Steels. Steels 1 to 4 Represent Increasing Niobium Contents. (After Morrison et al Ref. 1)
- Figure 2 : The Influence of Niobium on the Yield and Tensile Stresses of an As-Rolled Low C-Mn Laboratory Made Steel. (After Morrison Ref. 2)
- Figure 3 : The Influence of Niobium on the Charpy V-Notch Impact Transition Temperature of an As-Rolled Low C-Mn Laboratory Made Steel. (After Morrison Ref. 2)
- Figure 4 : Effect of Finishing Temperature on the Properties of 1.5% Mn - 0.06% Nb Steels. (After Duckworth et al Ref. 7)
- Figure 5 : Reprecipitation of AlN. Samples have been Solution Treated at 1350°C Then Quenched and Reheated at the Temperatures Shown. Precipitation is Rapid in Ferrite but Slow in Austenite. (After Duckworth et al Ref. 8)
- Figure 6 : Dissolution of Aluminium Nitride in High Aluminium/Nitrogen Steels. (After Nakamura Ref. 18)
- Figure 7 : Relation Between 15 ft.lb. Transition Temperature and AlN in Various Heat Treated 0.15% Carbon I N Steel. (After Nakamura Ref. 18)
- Figure 8 : Effect of Transformation Temperature on Grain Size and Yield Strength. (After Gray Ref. 15)
- Figure 9 : Effect of Manganese Content on Transformation Temperature. (After Gray Ref. 15)
- Figure 10. : Point Heat Source Moving on a Thick Plate (Ref. 22)
- Figure 11 : Line Heat Source Moving on a Thin Plate. (Ref. 22)
- Figure 12 : Value of B_{3D} as a Function of Temperature. (After Graville Ref. 22)
- Figure 13 : Graph to Determine Cooling Rate in Bead-On-Plate for Submerged-Arc Process. (Ref. 22)

- Figure 14 : Graph to Determine Cooling Time in Welds.
- Figure 15 : Double Peaked Temperature History in Concave Region of the Heat-Affected-Zone. (After Heuschkel Ref. 24)
- Figure 16 : Dimensionless Temperature Maximum Vs. Dimensionless Distance for Two Dimensional Heat Flow. (After Myers et al Ref. 24)
- Figure 17 : Dimensionless Temperature Maximum Vs. Dimensionless Distance for Three Dimensional Heat Flow. (After Myers et al Ref. 24)
- Figure 18 : Effect of Energy Input on the Maximum Austenite Grain Size in the Heat-Affected-Zone. (Ref. 22)
- Figure 19 : Influence of Bead Shape on Austenite Grain Size in the Heat-Affected-Zone.
- Figure 20 : Dependence of the Average Austenite Grain Size in Relation to Peak Temperature and Holding Time After Rapid Heating (100°C/s). (After Schmidtman. Ref. 26)
- Figure 21 : Typical Continuous Cooling Transformation Diagram for Simulated HAZ. A to F Represent Decreasing Cooling Rates Corresponding to Standard Welding Conditions. (After Watkinson Ref. 30)
- Figure 22 : Typical Hardening Curves for Two Types of Steel. (Ref. 22)
- Figure 23 : Free Energy of Formation of Carbides and Nitrides. (Ref. 20)
- Figure 24 : Equilibrium Solubilities of Carbides and Nitrides in Austenite. (Ref. 20)
- Figure 25 : The Solubility Product of CbC in Alpha-Iron Estimated From the Response of Yielding Behaviour to Annealing Temperature for Columbium-Treated Steels. (After Hook et al Ref. 12)
- Figure 26 : Equilibrium Stability of Niobium (Columbium) Carbonitride in Austenite. (After Cryderman Ref. 14)
- Figure 27 : Effect of Soluble Nitrogen on Impact Properties. (After Irvine Ref. 7)

- Figure 28 : Transition Temperature in $^{\circ}\text{F}$ vs. Peak Temperature in $^{\circ}\text{F}$. Distance from Weld Fusion Line to Indicated Temperature is also Shown. (After Aronson Ref. 41)
- Figure 29 : Results of Fracture Toughness Tests on Niobium Treated, Low Carbon Manganese Steels. (After Kaae, Ref. 43)
- Figure 30 : Test Results for Simulated and Weld HAZ Specimens. Grain Coarsened Region. (After Dolby Ref. 44)
- Figure 31 : COD Transition Curves for Parent Material and As-Welded Transformed Grain-Coarsened HAZ of a 1 kJ/mm Weld on Two C-Mn Steels. (After Saunders Ref. 40)
- Figure 32 : Variation of HAZ Hardness in Steel Containing Vanadium with a Holloman-Jaffe Time/Temperature Parameter. (After Saunders Ref. 40)
- Figure 33 : Transition Curves From Grain Coarsened HAZ's; C-Mn 0.056% Nb Steel. (After Cane et al Ref. 47)
- Figure 34 : Fracture Toughness of Martensitic Structures of Varying Prior Austenite Grain Size; Specimen Size 10 mm Square Section x55 mm. (After Dolby and Knott Ref. 48)
- Figure 35 : Variation of Prior Austenite Grain Size, Martensite Lath Width and Colony Width with Peak Temperature During Heat Treatment. (After Dolby and Knott Ref. 48)
- Figure 36 : Transition Temperature for a C-Mn Steel in Normalized and in As-Welded Simulated Condition Showing Effect of Niobium Content. (After Hannerz Ref. 49)
- Figure 37 : Influence of Vanadium on the Simulated Heat-Affected-Zone Transition Temperature after Hannerz and Jonsson-Holmquist. (After Hart Ref. 51. Data From Ref. 50 & 52)
- Figure 38 : Charpy Impact Toughness of Fusion Line at -20°F (-29°C), Plotted Against Columbium Content of Base Plates. (After Wada Ref. 53)
- Figure 39 : Impact Transition Curves for Full Size Charpy Impact Specimens Notched in the "50/50" Position of Mo-Cb Steel Welds. (After Sawhill Ref. 55)

- Figure 40 : Relationship Between Formula of Susceptibility in Steel for Bond Brittleness (PBA) and Measured Charpy Transition Temperature vTs of Welded Bond When Quenched Microstructure of Martensites and Lower Bainite were Formed in the Cooling Time on the Critical Range of About 11 sec. (After Ito et al Ref. 62)
- Figure 41 : Relationship Between Formula of Susceptibility in Steel for Bond Brittleness (PBB) and Measured Charpy Transition Temperature vTs of Welded Bond When the Intermediate Microstructure of Upper Bainites and Ferrites were Formed in the Cooling Time on the Critical Range of About 50 sec. (After Ito et al Ref. 62)
- Figure 42 : The Relation Between $T_{0c} = 0.1$ and C Content. The Vertical Axis is the Transition Temperature for a Critical Crack Opening Displacement (COD) of 0.1 mm and Represents the Toughness in Slow Loading Conditions. (After Miyoshi et al Ref. 63)
- Figure 43 : Toughness of Synthetic Weld Heat-Affected-Zone. The Parent Material Properties Have Been Changed by the Rolling Schedule. (After Shiga et al Ref. 64)
- Figure 44 : Variation of Yield Load Fracture Transition Temperature with Niobium Content for Four Heat Inputs: Lowest Heat Input is on 25 mm Plate. Cooling Times From 800-500°C Shown in Brackets. (Ref. 65)

1. INTRODUCTION

When a metal is welded by a fusion welding process part of the metal is melted and beyond this there is a heated region where temperatures up to the melting point are experienced. In a steel, the thermal cycles experienced by this heat-affected-zone (HAZ) will, in most cases, lead to changes in the properties of the material. These changes may have serious consequences, including cracking of the HAZ, loss of toughness leading to brittle fracture or loss of corrosion resistance. It is, therefore, essential to develop the physical metallurgy of the HAZ so that these changes can be predicted and appropriate courses of action taken in engineering applications.

Although many of the phenomena are understood in general terms by application of traditional metallurgical principles, few have a firm quantitative basis. For example, although the fast cooling rates in welds are known to produce martensitic microstructures of high hardness and that these effects are affected by alloy content, models for predicting heat-affected-zone hardness are not nearly as well developed as hardenability models are for conventional heat treating. There is, therefore, much progress to be made in developing the quantitative metallurgy of the HAZ to provide the basis on

which welding engineers can predict HAZ properties and select welding procedures.

This report presents a review of the more important references in the literature on metallurgical effects in the heat-affected-zone with particular emphasis on the fracture toughness of modern steels. It is appropriate to briefly describe the development of steels and in particular modern microalloy steels and their related weldability.

2. DEVELOPMENT OF STEELS

2.1. Steels and Weldability

The development of steels for structural purposes has been influenced by two main factors:

- (a) The advent of welding as the major method of joining materials, and
- (b) A greater understanding of the problem of brittle fracture which assumes greater importance as structures increase in size and members increase in thickness.

Early steels relied for their strength on the carbon content and a wide range of strengths could be obtained by utilizing different carbon contents. These materials were satisfactory for structural purposes when riveting and bolting were the primary methods of connection but with the advent of welding, a problem of heat-affected-zone cracking arose. Furthermore, the fracture toughness of the material became more important since structures were then continuous. The heat-affected-zone cracking problem was related to the fact that the thermal cycle involved in welding was rapid enough to cause hardening in the heat-affected-zone which, in the presence of hydrogen, resulted in gross cracking. The tendency to harden in the heat-affected-zone increased with the amount of carbon. The mechanical properties of the weld, however, were generally satisfactory. When the hard heat-affected-zones were avoided the strength and toughness of the heat-affected-zone and of the weld metal in general were superior to the parent material. Because the heat-affected-zone cracking problem was the major problem in welding steels of this type, the term "weldability" of a steel is often taken to mean the ease with which the steel can be welded without heat-affected-zone cracking. The term "ease" may be interpreted as meaning the degree to which one can omit the precautions (such as level of preheat) that must be applied to avoid cracking.

Recognition of the effect of carbon upon "weldability" and fracture toughness led steel makers to develop steels with lower carbon. Initially this has been done by addition of alloying elements such as manganese and silicon that contribute to the strength by solid solution hardening and later by increasing the hardenability of the steel such that heat treated, i.e., quenched and tempered materials, could be developed. The development of lower carbon steels, coupled with the development of low hydrogen electrodes has enabled most of these steels to be readily welded without problems, at least in thin sections. Preheat is generally required only in thicker sections and when the restraint is high. Steel makers now loosely describe their materials as being "weldable." Because quenched and tempered materials depend for their properties on careful heat treatment, it is to be expected that a problem may exist in welding because of the particular thermal cycle of the weld. In fact, loss of strength and deterioration of toughness may occur in the heat-affected-zone if the energy input of the weld is too large. For this reason, restrictions on energy input are often required when welding quenched and tempered materials.

2.2. Micro Alloy Steels

The demand for steels of good weldability and good low temperature toughness has prompted the development of new types of steel that have generally become known as high strength low alloy or micro alloy steels. The recognition of the role of carbon as an undesirable element from the point of view of weldability and low temperature toughness, demands that alternative strengthening mechanisms be found for the steel. Except for grain refinement, all strengthening mechanisms result in a decrease in toughness. Grain refinement, on the other hand, results in an increase in strength and an improvement in toughness, and there is general agreement that to meet the requirements of strength and toughness of modern-day service, fine grained steels are required.

Development in the Arctic regions of North America has underlined the need for steels of high strength with very good toughness. For example, pipelines carrying gas require high strength and very good toughness at low temperatures, since the consequences of failure would be extremely serious. Because of the quantities of steel required for such applications, conventional low temperature materials that rely on high levels of alloying elements, such as nickel, are

prohibitively expensive. Thus micro alloy steels become an economical alternative. This term is now generally applied to those high strength low alloy steels that derive properties from the use of low levels of certain alloying elements that contribute to grain refinement or precipitation hardening. This distinguishes them from those steels that use higher levels of alloy elements for solid solution hardening or effecting microstructural changes by increasing hardenability.

Although the effects of small additions of niobium on strength have been known for a long time, it is only in the last fifteen years that economically available niobium has allowed full exploitation of this element in steel. This period has been marked by extensive research on the effects of micro alloy elements. The effects of aluminium and titanium additions on grain size in normalized steels and strengthening effects of vanadium have also been known for a long time, but these too have been extensively studied in recent years. Another important factor in modern micro alloy steels is the use of controlled rolling. Again, this has been practised for many years to improve toughness, but only as a result of recent research has it been included as an integral part of the metallurgical design of steels.

Work on the effect of niobium⁽¹⁾ showed that with high austenitizing temperatures (or conventional rolling), the strengthening effect resulted mainly from precipitation hardening. There was no effective grain refinement. In this condition, steels would show an increase in strength with increasing niobium content but a decrease in fracture toughness⁽²⁾. (See Figures 1, 2 and 3.)

With lower austenitizing temperatures, grain refinement was the major contributor to strength. Grain refinement would increase strength and fracture toughness⁽³⁾, (Figure 4). If the steel was rolled with a low finishing temperature strength could be increased by both grain refinement and coherent precipitation in the ferrite during cooling⁽⁴⁾⁽⁵⁾. Normalizing a niobium steel would result in grain refinement but the coherency of any precipitation in the ferrite would be lost and the solubility of the niobium at normalizing temperatures would be insufficient to produce new precipitation on cooling. This is illustrated in Figure 1, where high austenitizing temperatures are required to dissolve the niobium to get coherent precipitation in the ferrite after cooling. At lower temperatures any precipitation in the austenite would result in a non-coherent dispersion and have only limited strengthening ability. Vanadium, however, has

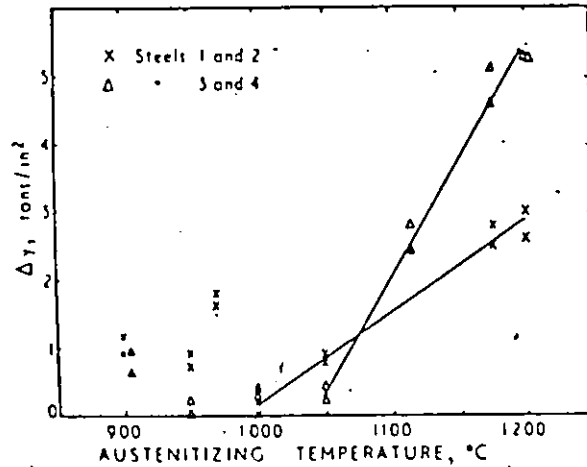


Figure 1 : Increase in Yield Stress, ΔY Plotted Against the Austenitizing Temperature of the Niobium Steels. Steels 1 to 4 Represent Increasing Niobium Contents. (After Morrison et al. Ref. 1)

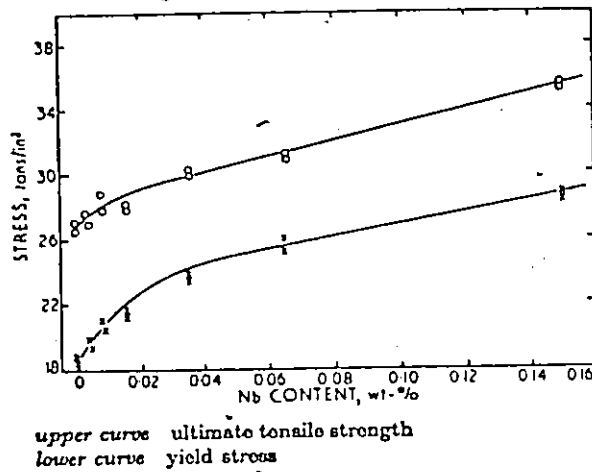


Figure 2 : The Influence of Niobium on the Yield and Tensile Stresses of an As-Rolled Low C-Mn Laboratory Made Steel. (After Morrison Ref. 2)

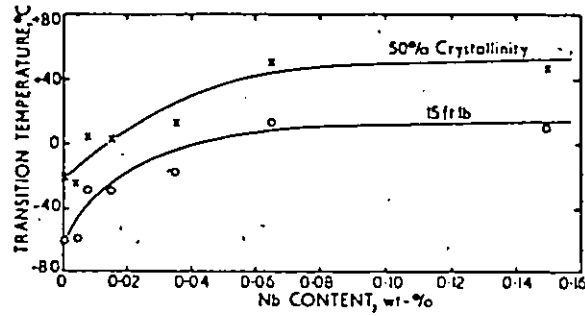


Figure 3 : The Influence of Niobium on the Charpy V-Notch Impact Transition Temperature of an As-Rolled Low C-Mn Laboratory Made Steel. (After Morrison Ref. 2)

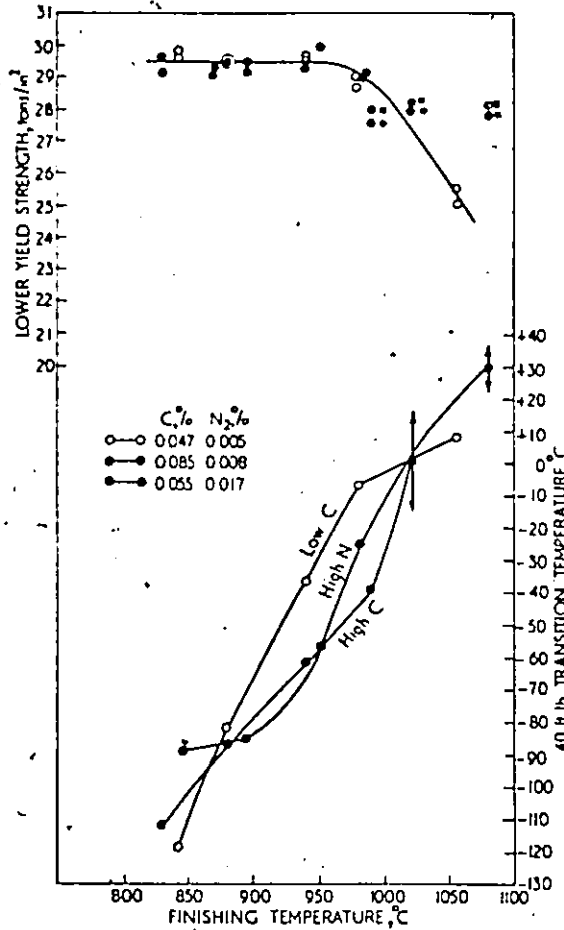


Figure 4 : Effect of Finishing Temperature on the Properties of 1.5% Mn - 0.06% Nb Steels. (After Duckworth et al. Ref. 7)

been shown⁽³⁾ to give significant strengthening through precipitation as well as grain refinement in a normalized steel. This results from the greater solubility at normalizing temperatures that allows reprecipitation on cooling.

Based on this appreciation of precipitation hardening and grain refinement, commercial steels were developed⁽⁶⁾ and Duckworth et al⁽⁷⁾ showed that low carbon steels with high yield and a low impact transition temperature could be produced. The importance of a low finishing temperature in rolling and sufficient draught in the final pass was demonstrated. Based on this work, attempts at commercial production of these "Pearlite Reduced" steels were made. The first serious evaluation of the welding behaviour of these steels was carried out at the British Welding Research Association (now The Welding Institute) and will be described later.

Aluminium has been used for many years as a grain refiner in normalized steels⁽⁸⁾. During reheat treatment, particles of aluminium nitride pin grain boundaries and retard grain growth. At temperatures above 1000°C, however, the aluminium nitride dissolves and grain coarsening occurs. Reprecipitation

is sluggish until transformation occurs (Figure 5) and in normal rolling, therefore, aluminium is ineffective in producing grain refinement⁽⁸⁾. Attempts have been made, notably in Japan⁽¹⁸⁾, to produce grain refinement in rolled aluminium steels. High nitrogen contents are used to increase the dissolution temperature and lower (about 1150°C) reheating temperatures for rolling are used (see Figures 6 and 7).

Titanium also acts as a grain refiner but its action is more complex. It also forms carbides (or carbonitrides) and the control of precipitate size is more difficult. There has been renewed interest in titanium in recent years and its possible effect in the heat-affected-zone of welds is discussed in a later section.

The disadvantage of aluminium and titanium is their high affinity for oxygen, which makes them useful only in fully killed steels. Niobium and vanadium, on the other hand, can be beneficial in semi-killed steels. A further advantage of niobium over the other grain refining elements is that it retards austenite recrystallization more than the others and this property makes it particularly useful in controlled rolling.

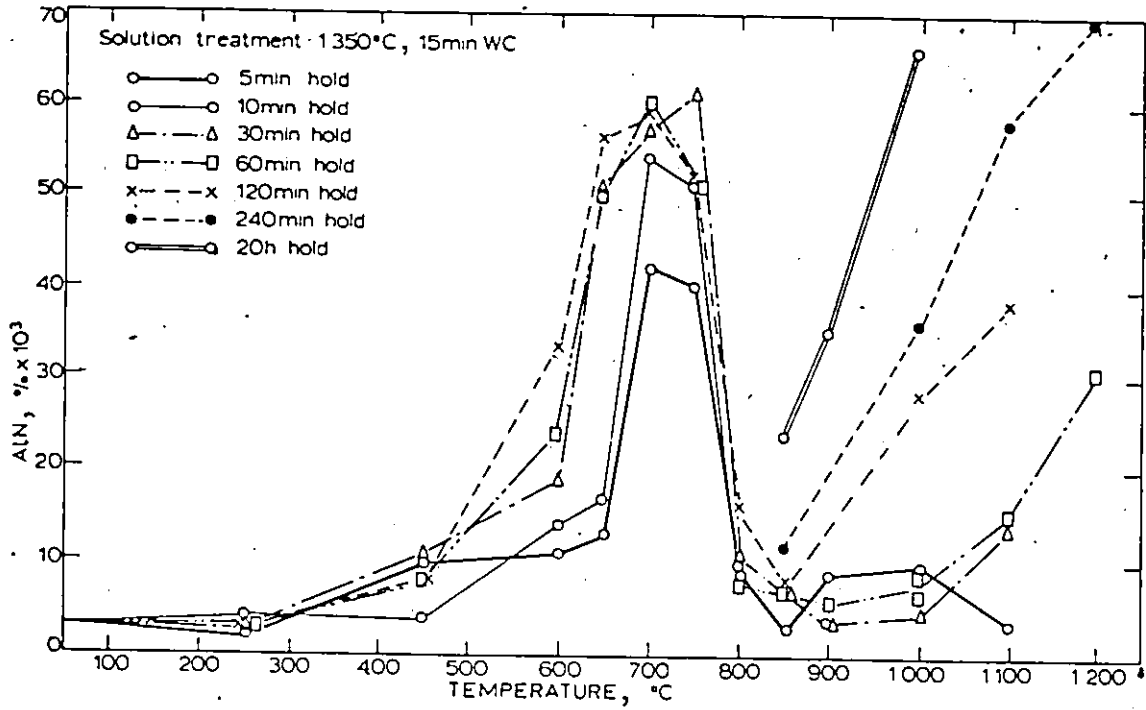


Figure 5 : Reprecipitation of AlN. Samples have been Solution Treated at 1350°C Then Quenched and Reheated at the Temperatures Shown. Precipitation is Rapid in Ferrite but Slow in Austenite. (After Duckworth et al. Ref. 8)

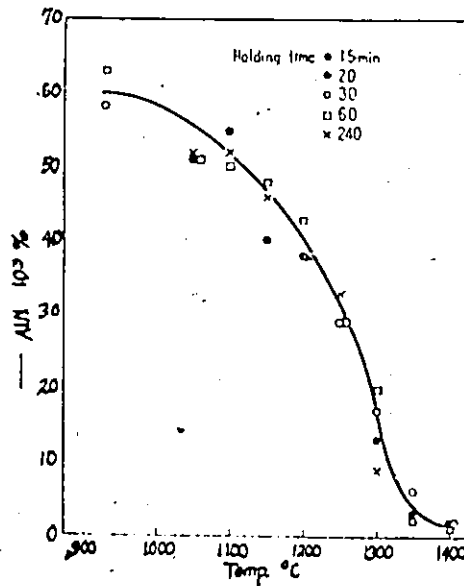


Figure 6 : Dissolution of Aluminium Nitride in High Aluminium/Nitrogen Steels. (After Nakamura Ref. 18)

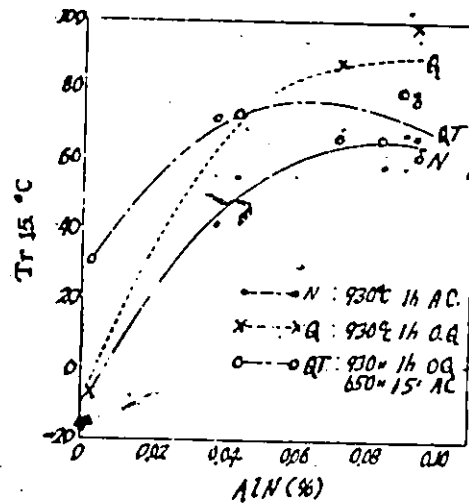


Figure 7 : Relation Between 15 ft.lb. Transition Temperature and AlN in Various Heat Treated 0.15% Carbon I N Steel. (After Nakamura Ref. 18)

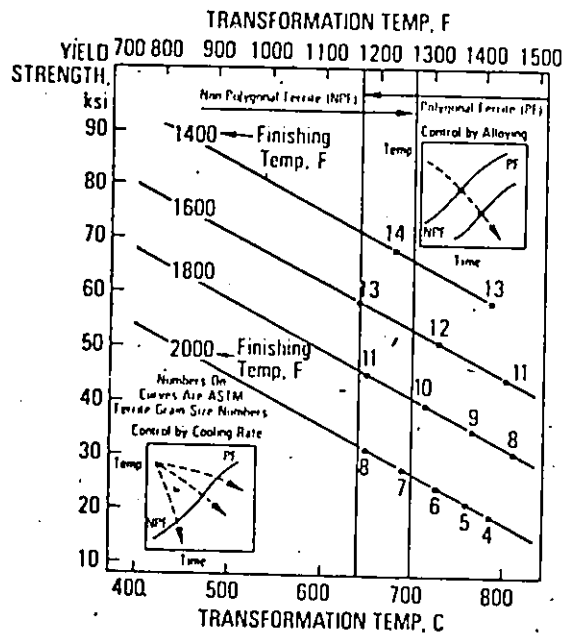


Figure 8 : Effect of Transformation Temperature on Grain Size and Yield Strength. (After Gray Ref. 15)

By 1970, it was possible for Irvine et al (10) to summarize the factors which will give the best properties. The most important factor was to obtain a small austenitic grain size. At least 50% deformation was required in the lower temperature region where re-crystallization and grain growth were restricted, although deformation should cease before transformation to ferrite. The carbon content should be as low as possible to restrict the pearlite content which has an adverse effect on toughness.

The steels described to this point derive their good properties from a fine ferrite grain size which is a legacy from the fine austenite grain size. The second factor which controls the grain size of the final product is, of course, the transformation temperature (Figure 8) and depression of the transformation by suitable alloying may further reduce the grain size (Figure 9). With increased alloying, transformation to other types of products (bainite, martensite) may occur.

In ferritic steels with low carbon, it was early appreciated that manganese should be as high as possible without forming bainite to depress the transformation temperature and levels of up to 2% (in low carbon steels) have been proposed.

TRANSFORMATION TEMPERATURES
ON COOLING, F

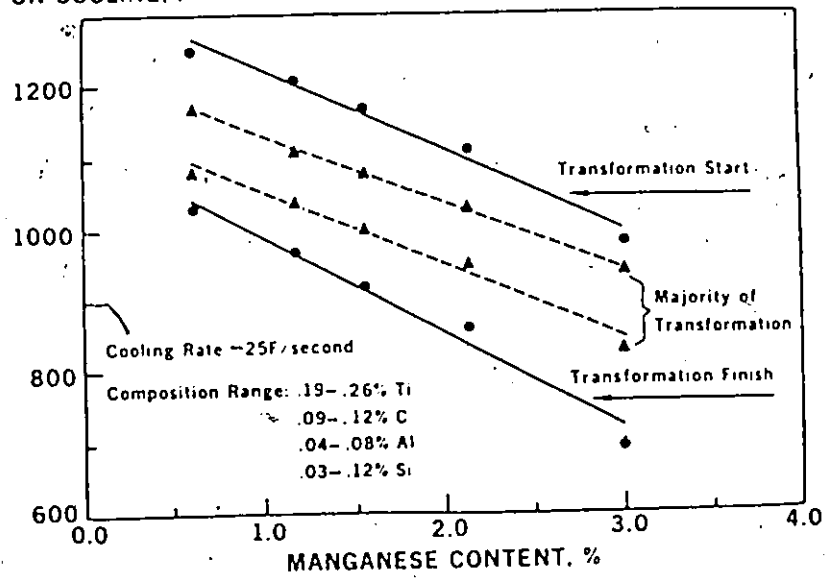


Figure 9 : Effect of Manganese Content on Transformation Temperature.
(After Gray Ref. 15)

Pickering⁽¹⁹⁾ has recently reviewed bainitic steels in which molybdenum and boron have been used. Early steels of this type did not have excellent toughness because of difficulty of maintaining low carbon and because controlled processing was still in its infancy. Recently, there has been much interest in steels with acicular ferrite microstructures where very good toughness levels have been achieved. To form an acicular ferrite, sufficient alloying is necessary to depress the transformation temperature and low carbon must be maintained. In some cases accelerated cooling has been used to depress the transformation⁽¹³⁾⁽¹⁷⁾.

3. THERMAL CONDITIONS IN THE HEAT-AFFECTED-ZONE

A study of the physical metallurgy of the heat-affected-zone requires an understanding of the thermal conditions existing there. Despite the importance of this, relatively few detailed experiments have been carried out to study temperature distributions. Precise theoretical calculations are lacking, although recent numerical methods are promising⁽²¹⁾. Of most significance in the HAZ is the peak temperature reached and the cooling rate, since these, to a large extent, control the microstructure. However, the retention times (i.e., time above a given temperature) and the temperature gradients may also be important in controlling metallurgical

phenomena. In this brief discussion the aspects of point source theory relevant to the HAZ are initially presented.

3.1. Point Source Theory

Welding can be approximately represented by a point source moving on the surface of a plate. For thick plate, the problem becomes three dimensional (Figure 10). For thin plate, a line source through the thickness of the plate is assumed, thus being equivalent to a two dimensional problem (Figure 11). For thick plate, the temperature distribution becomes:

$$T - T_0 = \frac{\dot{Q}}{2\pi k} \cdot \frac{1}{r} \exp -\lambda v(r+\xi) \quad (1)$$

where the terms are defined at the end of the report. For 2-D (thin plate):

$$T - T_0 = \frac{\dot{Q}}{2\pi k g} \exp (-\lambda v \xi) K_0(\lambda v r) \quad (2)$$

The equations can be differentiated to give the cooling rates on the weld centreline. For thick plate conditions (3-D heat flow):

$$-\frac{\partial T}{\partial t} = \frac{2\pi k v}{\dot{Q}} (T - T_0)^2 \quad (3)$$

and for thin plate (2-D at flow):

$$-\frac{\partial T}{\partial t} = \frac{2\pi k \rho C_g^2 v^2}{\dot{Q}^2} (T - T_0)^3 \quad (4)$$

Since the physical constants (k , λ) are assumed to be independent of temperature, discrepancies will arise due to the variation of the real values with temperature. This has led a number of investigators to take the theoretical form of the cooling rate equations and determine the constants empirically. For example, Graville⁽²²⁾ writes the thick plate cooling rate as

$$\frac{\partial T}{\partial t} = B_{3D} \frac{(T - T_0)^2}{E} \quad (5)$$

where the empirical constant B_{3D} was determined as a function of temperature and is shown in Figure 12. This enables cooling rates to be determined from simple graphs. Graphs for cooling rates in submerged-arc bead-on-plate welds are shown in Figures 13 and 14. At high energy inputs and thin plates, heat loss by surface transfer becomes significant and this is reflected in the shape of the curves for these conditions in the graph.

Several temperatures have been suggested at which the cooling rate should be measured. It is now generally agreed that if transformation is of interest, then a temperature (or temperature range) close to that at which transformation

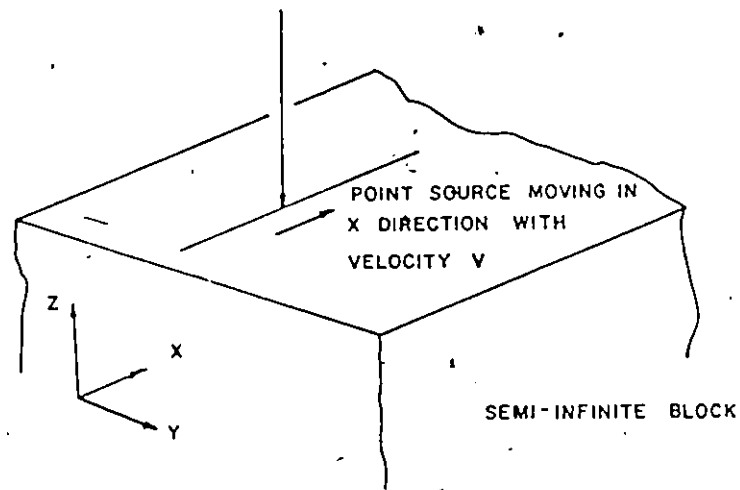


Figure 10 : Point Heat Source Moving on a Thick Plate (Ref. 22)

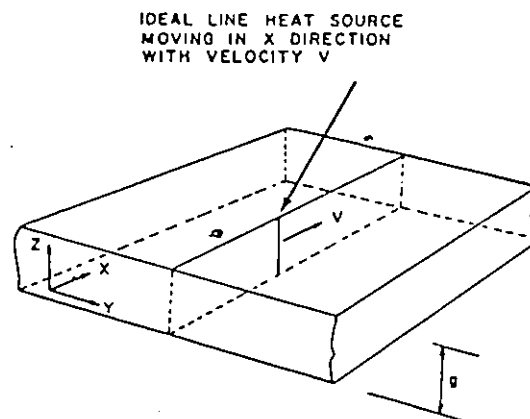


Figure 11 : Line Heat Source Moving on a Thin Plate (Ref. 22)

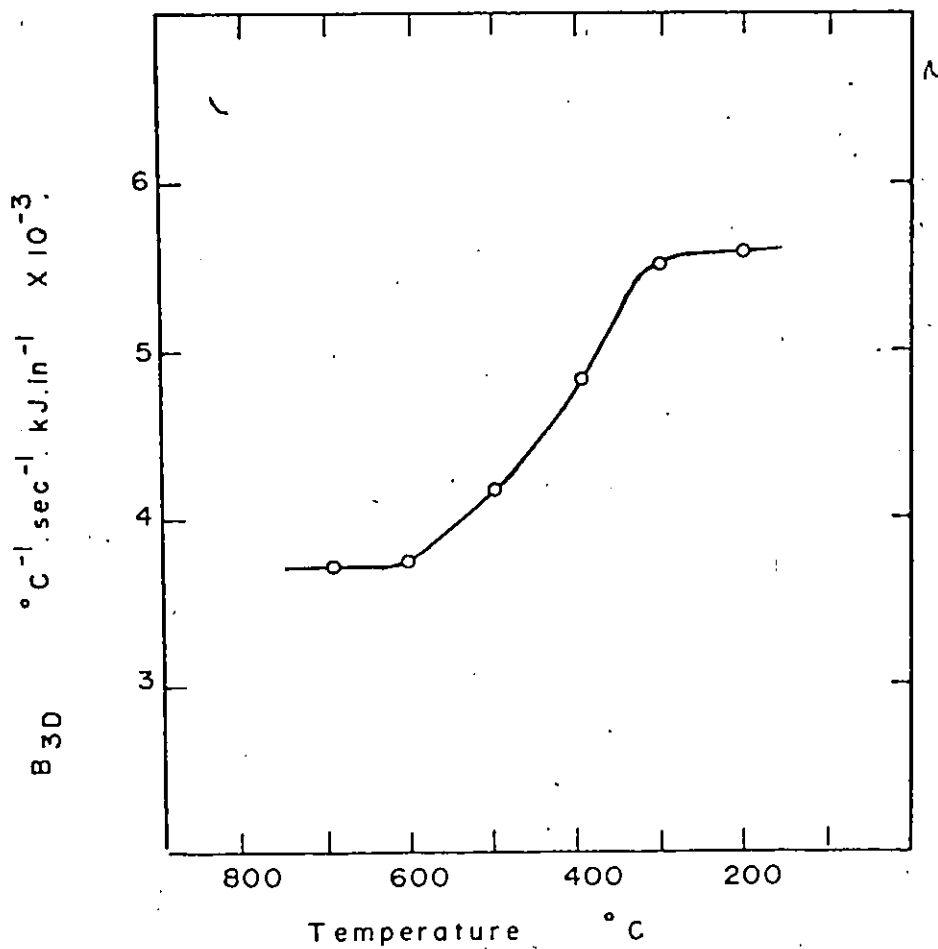


Figure 12 : Value of B_{3D} as a Function of Temperature. (After Graville Ref. 22)

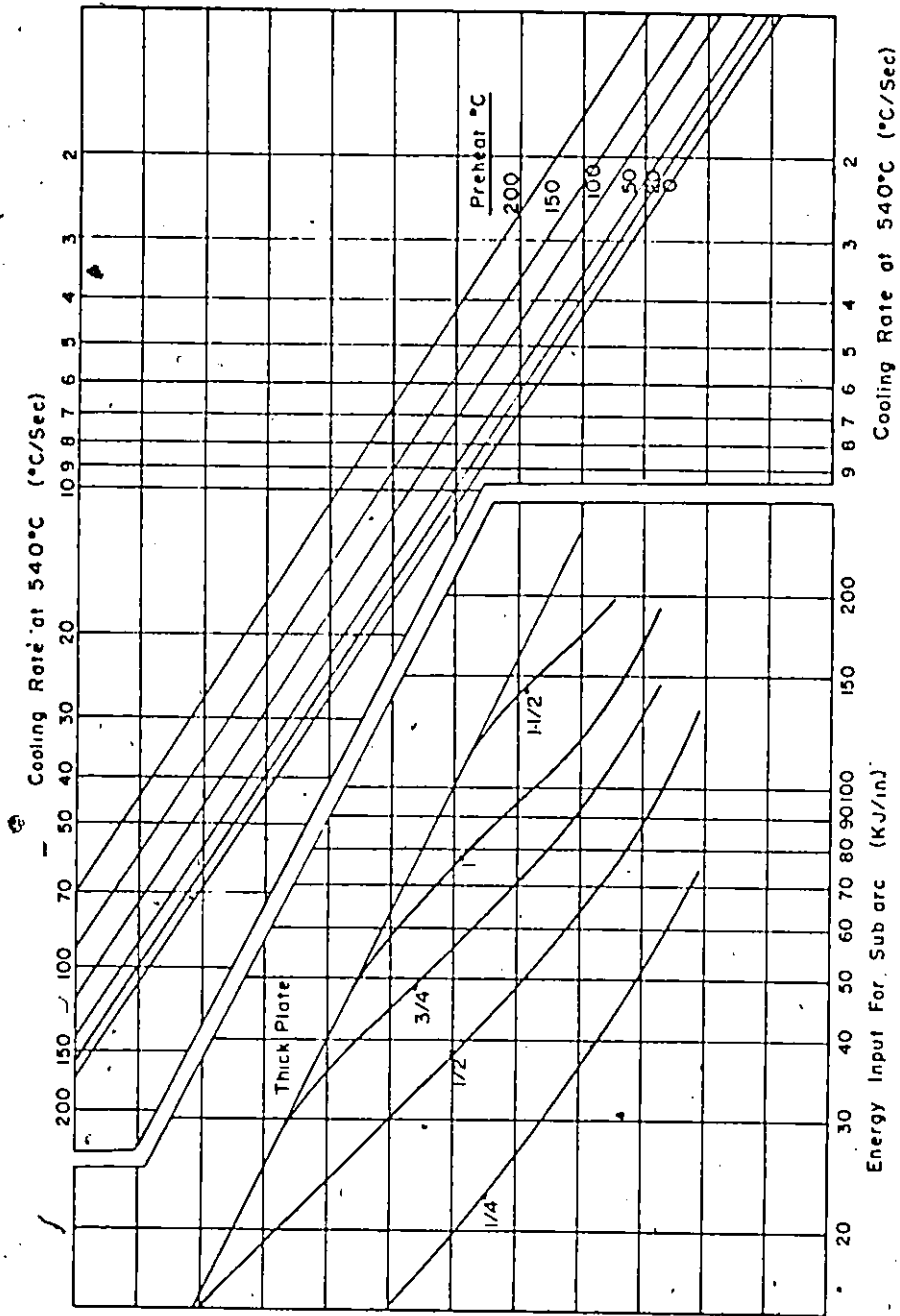


Figure 13 : Graph to Determine Cooling Rate in Bead-On-Plate for Submerged-Arc Process. (Ref. 22)

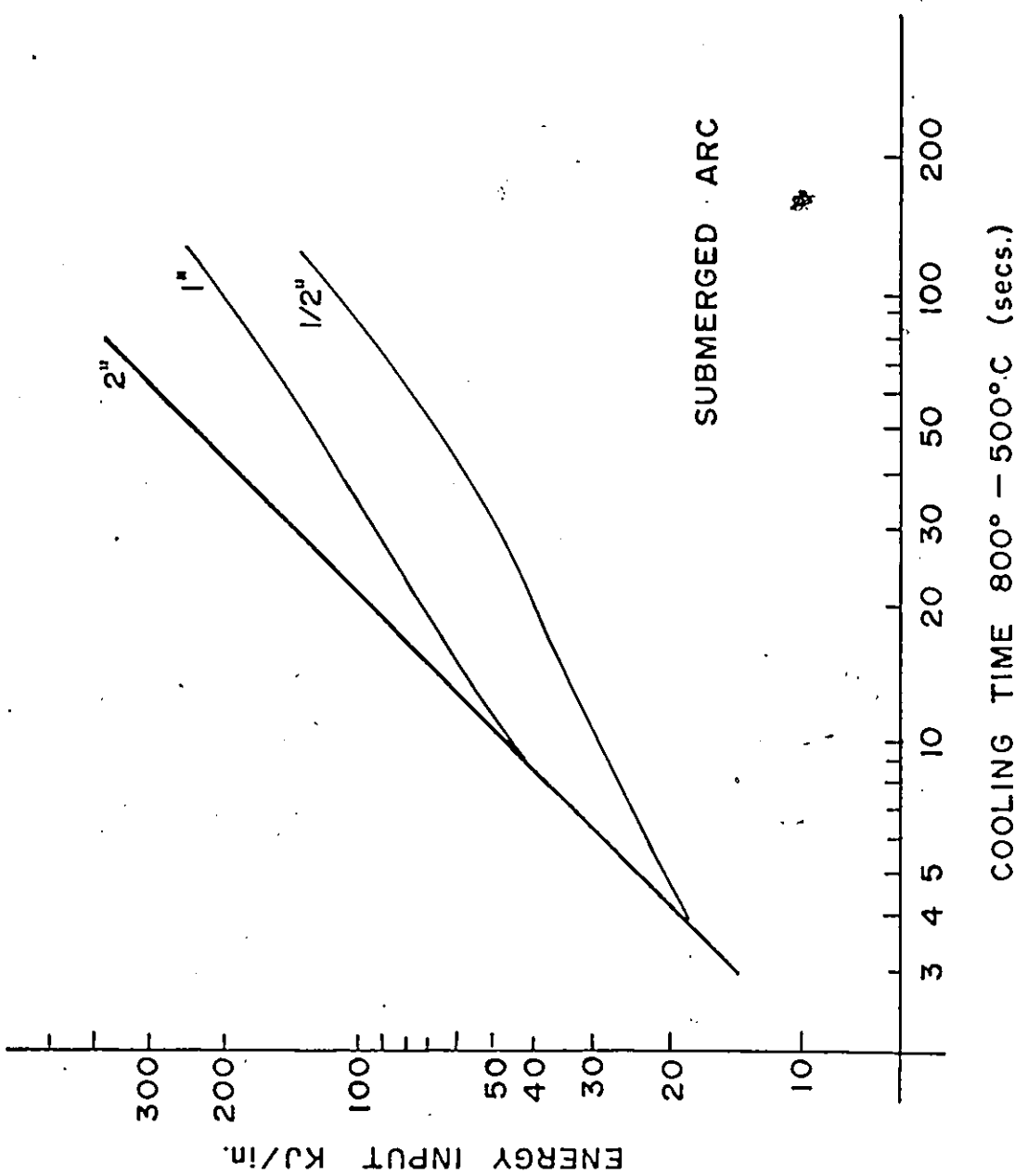


Figure 14 : Graph to Determine Cooling Time in Welds.

occurs is most suitable. Thus, for general use, cooling rate at 540°C or cooling time $800-500^{\circ}\text{C}$ is applicable. If hydrogen cracking is of interest, hydrogen diffusion is important and the cooling rate in the lower temperature range (e.g., $300-100^{\circ}\text{C}$) becomes a useful parameter.

The temperature at which to measure cooling rate has been correlated with hardness for a particular steel⁽²³⁾ and it was found that for hardness up to 375 H_V , a temperature between $400-500^{\circ}\text{C}$ was the most accurate, but for hardnesses above this, where the HAZ was largely martensitic, the temperature dropped to about 300°C .

The cooling rates given refer to the weld cooling rate. Few accurate measurements in the HAZ have been made, largely because of experimental difficulties. From theoretical considerations, it may be shown that the cooling rate during transformation (below 700°C) in the region that exceeded about 900°C (i.e., the transformed region) will be approximately the same as the centre of the weld. For practical purposes, therefore, a single weld cooling rate measured on the weld centreline may be used to characterize the entire weld that exceeds about 900°C .

Point source theory is quite useful at distances away from the source, i.e., at lower temperatures, but is inaccurate close to the arc at high temperatures. One problem is that it does not take account of melting. The distributed heat source in a real arc may also result in a fusion boundary which is not semi-circular (3-D) or linear (2-D) as expected from point source theory. Although the theory may be useful for estimating the width of the heat-affected-zone, it does not accurately give the temperature distribution close to the fusion boundary. For example, measured temperature histories in the concave region (see Figure 19) of the fusion boundary of a gas shielded weld show a double peak (Figure 15).

Peak temperatures may readily be determined from the theory. For the two dimensional case, the results are presented in Figure 16. The width of HAZ between two isotherms (say the melting temperature and some other) is approximately given for the 2-D case by:

$$Y_m - Y = \frac{C}{\lambda r (kg/Q)}^{1/n_2} \left[\frac{1}{(\Theta_{2m})^{1/n_2}} - \frac{1}{(\Theta_{2max})^{1/n_2}} \right] \quad (6)$$

where n_2 is an index close to unity. Thus, the width of the HAZ in the 2-D case is approximately proportional to the heat input. For the 3-D case, the results are given in Figure 17. The distance from the point source is $b = \sqrt{Y^2 + z^2}$ and is the

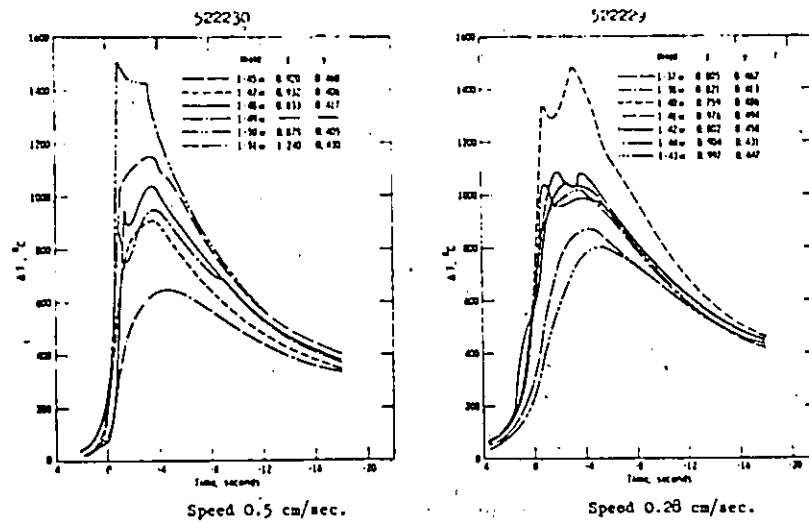


Figure 15 : Double Peaked Temperature History in Concave Region of the Heat-Affected-Zone. (After Heuschkel Ref. 24)

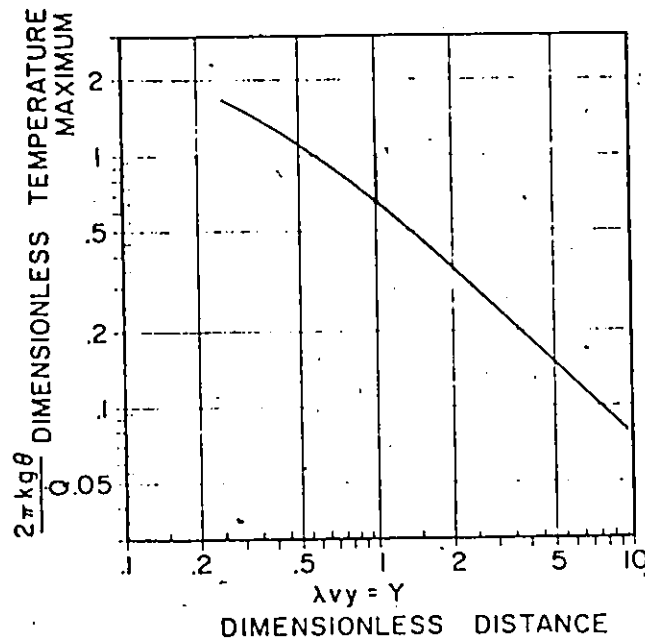


Figure 16 : Dimensionless Temperature Maximum Vs. Dimensionless Distance for Two Dimensional Heat Flow. (After Myers et al. Ref. 24)

radius in the Y, z plane. The width of the heat-affected-zone is similarly given by:

$$b_m - b = \frac{\text{Const.}}{\lambda v (k/Q\lambda v)}^{1/n_3} \left[\frac{1}{(\Theta_{3m})}^{1/n_3} - \frac{1}{(\Theta_{3\max})}^{1/n_3} \right] \quad (7)$$

where $n_3 = 1.70$ and the width varies in a more complex manner with heat input. It is of interest to note that in the case of 2-D heat flow, the width of the HAZ depends on the heat input $H = Q/v$ only and not on welding speed separately. In the 3-D case, however, the width of HAZ will depend on the heat input and the welding speed.

In real welds the fusion boundary is not usually semi-circular and these equations will not be very accurate. In the concave region, the HAZ is wider and the temperature gradient less steep than in the convex region.

3.2. Grain Coarsening

When steels are welded, a region of the HAZ will transform to austenite and grain growth can occur. It is well-known that the extent of grain growth depends on the energy input of the welding process and typical results are shown in Figure 18.

In very high heat input welds (such as electroslog), the austenite grains can grow to their equivalent isothermal size.

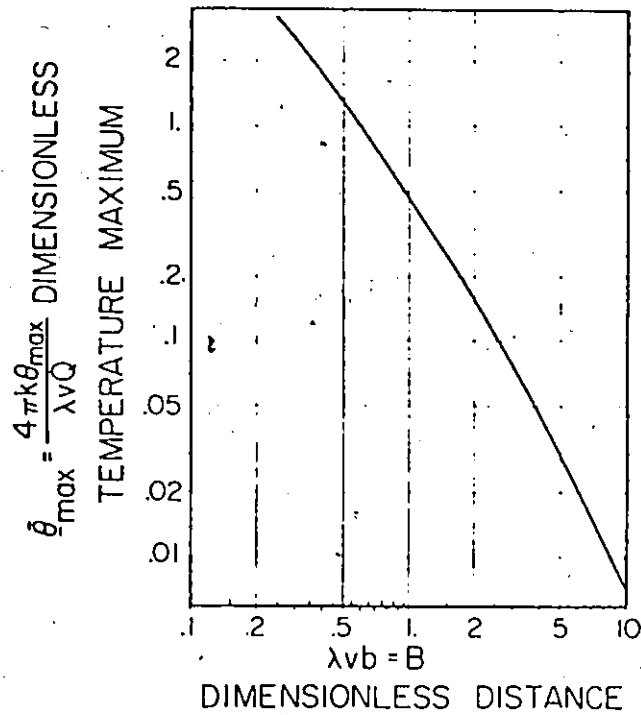


Figure 17 : Dimensionless Temperature Maximum Vs. Dimensionless Distance for Three Dimensional Heat Flow. (After Myers et al. Ref. 24)

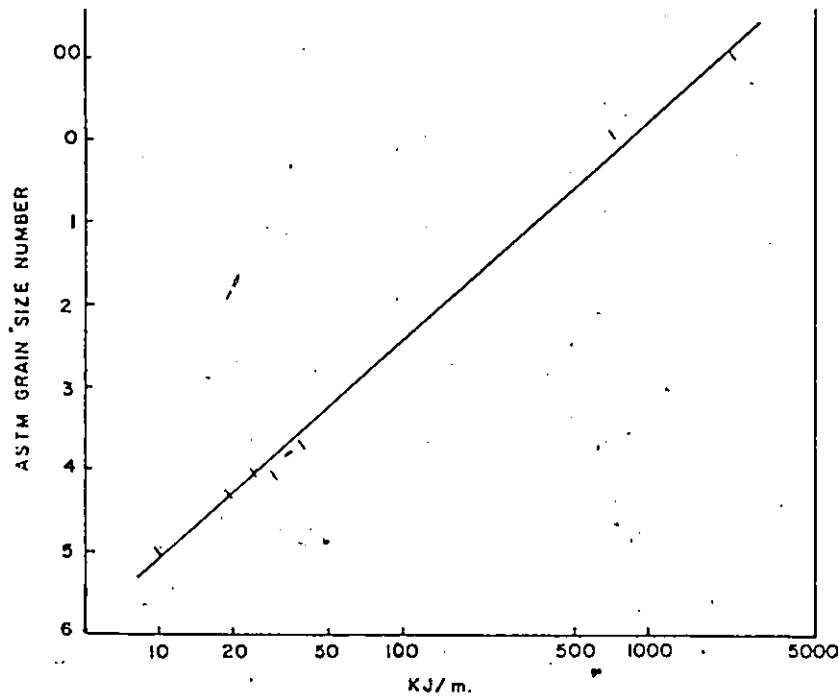


Figure 18 : Effect of Energy Input on the Maximum Austenite Grain Size in the Heat-Affected-Zone. (Ref. 22)

This is the grain size that would be quickly attained in a specimen uniformly heated to the same temperature. It might be expected, therefore, that the grain size in very high energy welds is independent of the energy input. In lower energy welds, the grain size may be controlled by the retention time and the temperature gradient in the HAZ. The latter is an important effect since it means that fusion boundary contour can influence grain size. In regions where the boundary is concave, a considerably larger grain than at convex regions may result (Figure 19). The width of HAZ and, therefore, the temperature gradient will also be influenced by whether the mode of heat transfer is two or three dimensional. Thus, for the same energy input, a smaller temperature gradient and larger grain size may be anticipated for thin material (2-D) as opposed to thick material. This effect may be significant if HAZ toughness considerations dictate the need for energy input limitations.

There have only been a few attempts to establish a quantitative model for grain growth in the HAZ. Maynier et al⁽²⁵⁾ have assumed that the effect of austenitizing can be related to a parameter which depends on the peak temperature and the retention time

$$P = \left(\frac{1}{T} - \frac{nR}{\Delta H} \log \frac{t}{t_0} \right)^{-1} \quad (8)$$

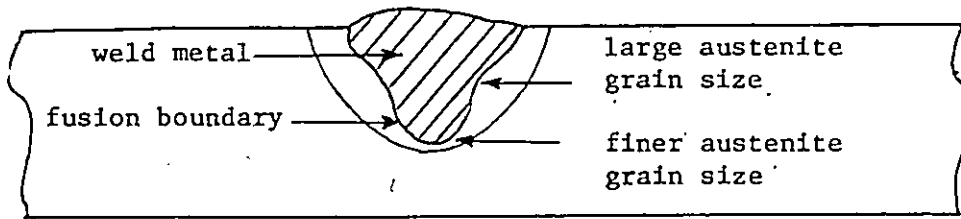


Figure 19 : Influence of Bead Shape on Austenite Grain Size in the Heat-Affected-Zone.

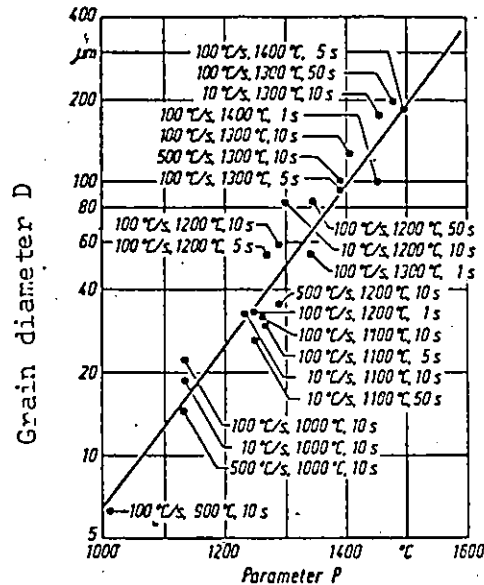


Figure 20 : Dependence of the Average Austenite Grain Size in Relation to Peak Temperature and Holding Time After Rapid Heating (100 °C/s). (After Schmidtman. Ref. 26)

Where: T = temperature °K

t_0 = time

t = time unit

ΔH = activation energy (110 kcals/mole for grain growth)

nR = constants

This parameter has been useful for comparing Continuous Cooling Transformation (CCT) curves where the peak austenitizing temperature differed. Schmidtman and Rippel⁽²⁶⁾ used this parameter to relate to the austenitic grain size in simulated specimens. Results are shown in Figure 20. Such a parameter does not take account of the precise thermal cycle or the temperature gradient in the HAZ and although it appears useful for simulated specimens, its usefulness for real HAZ's has yet to be demonstrated.

Ikawa, Shin and Oshiga⁽²⁷⁾ studied grain growth in nickel during thermal cycles representing welding. They found that the amount of grain growth during a thermal cycle could be predicted by dividing the cycle into steps and summing the amount of growth during each isothermal step. Grain size was given by:

$$(D_{i-1})^a = k_0 \sum_{e=1}^{i-1} \Delta t_e \exp \left(-\frac{Q}{RT_e} \right) + (D_0)^a \quad (9)$$

Where: D_{i-1} = grain size at T_i ($^{\circ}\text{K}$) during thermal cycle (D in mm.)
 D_0 = initial grain size
 t_e = time (min.) at T_e
 a, k_0, Q = material constants (R = gas constant).

Again, such an approach assumes a uniform temperature and that grain size depends solely on the thermal cycle and not the temperature gradient. Application of this to a real HAZ has not been demonstrated. In a real weld the growth of a grain is restricted by the fact that a moving grain boundary will move into a region at a different temperature. As the temperature gradient becomes steeper the distance between two given isotherms becomes smaller and decreases relative to the grain size that would be achieved in a uniform temperature field. Temperature gradient then becomes the controlling factor as illustrated in Figure 19. The work of Ikawa et al provides a good basis for further work on real HAZ's and the establishment of a model to predict grain size in the HAZ would be a useful field of endeavour.

4. HARDNESS OF THE HEAT-AFFECTED-ZONE

This property is of great importance in the welding of steels mainly because of the effect on hydrogen cracking. Early work⁽²⁸⁾ associated

cracking with the formation of hard (martensitic) microstructures which would be highly susceptible to hydrogen embrittlement.

Cracking could be controlled by modifying the cooling rate so that such microstructures were not formed. One of the first attempts to quantify the hardening behaviour of the HAZ was by Stout and co-workers⁽²⁹⁾. He attempted to relate the behaviour in the HAZ to the conventional hardenability as determined in a Jominy test. The cooling rate in the Jominy specimen is a function of the distance from the end, so by measuring this distance, the cooling rate to produce a particular hardness can be found. This cooling rate can be related to the welding parameters or size of weld and hence enable HAZ hardness to be controlled. The approach has not been widely used and there are a number of reasons why accurate results would not be expected. The main difference between the HAZ and the Jominy test is the austenitizing conditions. The peak temperatures are higher in the HAZ and this affects both grain size and solubility of second phases. In addition, the grain size is further influenced by the temperature gradient.

Work at BWRA (Welding Institute)⁽³⁰⁾ and elsewhere⁽³¹⁾ has been aimed at establishing the hardenability behaviour in the HAZ by producing continuous cooling transformation (CCT) diagrams (Figure 21).

Recognizing the effect of peak temperature, values of about 1350°C have usually been utilized. The techniques have usually involved

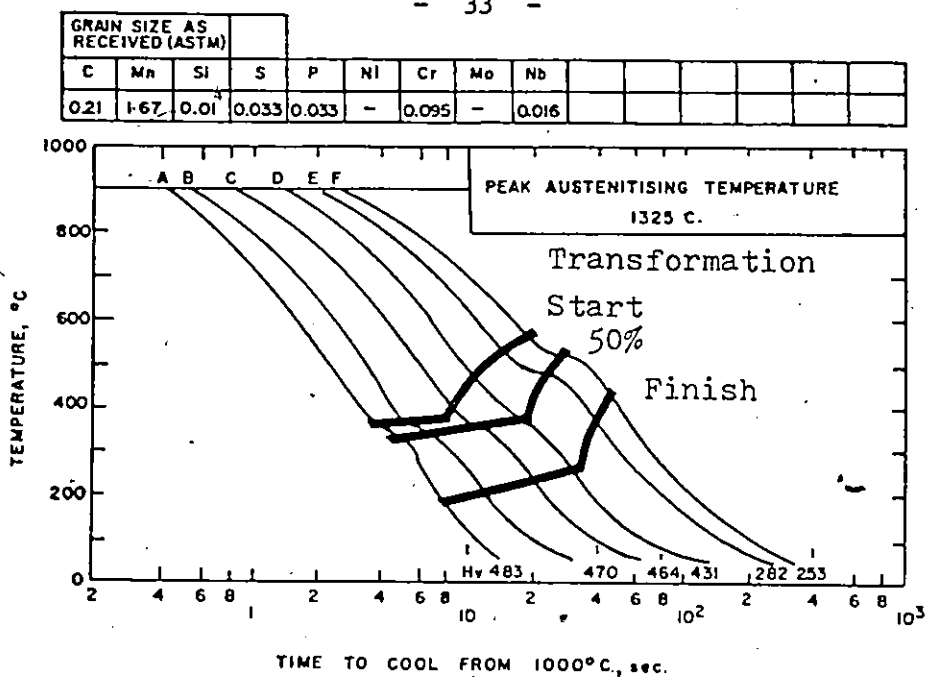


Figure 21 : Typical Continuous Cooling Transformation Diagram for Simulated HAZ. A to F Represent Decreasing Cooling Rates Corresponding to Standard Welding Conditions. (After Watkinson Ref. 30)

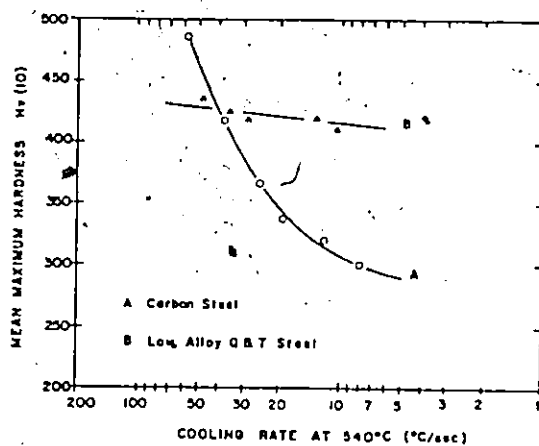


Figure 22 : Typical Hardening Curves for Two Types of Steel. (Ref. 22)

dilatometry⁽³⁰⁾ although thermal analysis has also been used⁽³²⁾.

These diagrams have been more useful than the Jominy approach and reasonable agreement with welding behaviour is found⁽³³⁾.

Other authors⁽²²⁾ have preferred to derive hardenability curves directly from welding experiments. In this case the hardness of the HAZ observed close to the fusion boundary where the grain size reaches a maximum, is plotted as a function of cooling rate. Such hardening curves are easily derived using simple methods where the cooling rate of the weld is known (Figure 22).

There has naturally been much interest in relating the hardening behaviour to the chemical composition of the steel and it is surprising that except for some recent work⁽³⁴⁾ the lines developed for predicting hardenability in conventional heat treatment have not been followed in welding. Part of the reason for this is that the concept of carbon equivalent which is a linear model of composition (the effect of alloys is additive) was quickly adopted to give a guide to "weldability," i.e., resistance to cracking. The carbon equivalent was originally related to the martensite start temperature and it was believed this controlled the crack susceptibility. Later work by Cottrell⁽³⁵⁾ showed that cracking could be related to a critical cooling rate measured at 300°C and it was also observed that cracking occurred when a critical hard-

ness was exceeded. An extensive study⁽³⁶⁾ of HAZ cracking at the British Welding Research Association (Welding Institute) resulted in a scheme⁽³⁷⁾ for predicting welding conditions that would not lead to cracking. The cooling rate at 300°C is controlled so that a critical hardness dependent on hydrogen content is not exceeded. The critical cooling rate for this hardness could be related to the composition of the steel through the carbon equivalent formula. This scheme has proved very useful although a number of problems exist with it. The choice of 300°C for the temperature at which to measure the cooling rate resulted in discrepancies when preheat was used. Preheat would affect the cooling rate at 300°C more than that at higher temperatures where transformation was occurring and higher hardness than expected was therefore observed.

The carbon equivalent chosen by Bailey for this system has been in use for many years, but a recent analysis⁽³⁴⁾ of a large number of hardening curves shows it to be a very good choice. There is, however, no fundamental or theoretical reason to select a linear model. In conventional heat treating, linear models were discarded more than thirty years ago and replaced by product models in the classic work of Grossman⁽³⁸⁾. A recent attempt⁽³⁴⁾ has been made to fit a product model to the welding data, but no improvement was shown. Part of the difficulty lies in the difference in definition of hardenability in the welding case (critical cooling rate for a

given hardness) as opposed to that conventionally used (critical cooling rate for 50% martensite). It is also expected that the product model would be more appropriate to a wide range of alloy contents, while most of the welding data covers only a very narrow range of compositions. This is clearly an area for further study.

5. MICROALLOY ELEMENTS IN THE HAZ

The free energy of formation of carbides and nitrides of the common microalloying elements is shown in Figure 23. Aluminium only forms a nitride, whereas with niobium the carbon and nitrogen are interchangeable over the whole range. In the case of steels containing more than one microalloy element there will be competition for the nitrogen. For example, if the aluminium content is high, all nitrogen will be tied up as AlN and the addition of vanadium will not produce many precipitates of vanadium nitride. The stability of the precipitates can be determined (under equilibrium conditions) from the solubility product. Since the elements are not usually present in stoichiometric quantities, the solubility of the precipitate will be controlled by the actual levels of the individual elements. Solubility products for carbides and nitrides in austenite are shown in Figures 24 and 26. Solubility is generally much lower in ferrite and the estimated solubility product for niobium carbide is shown in Figure 25. From the solubility data it

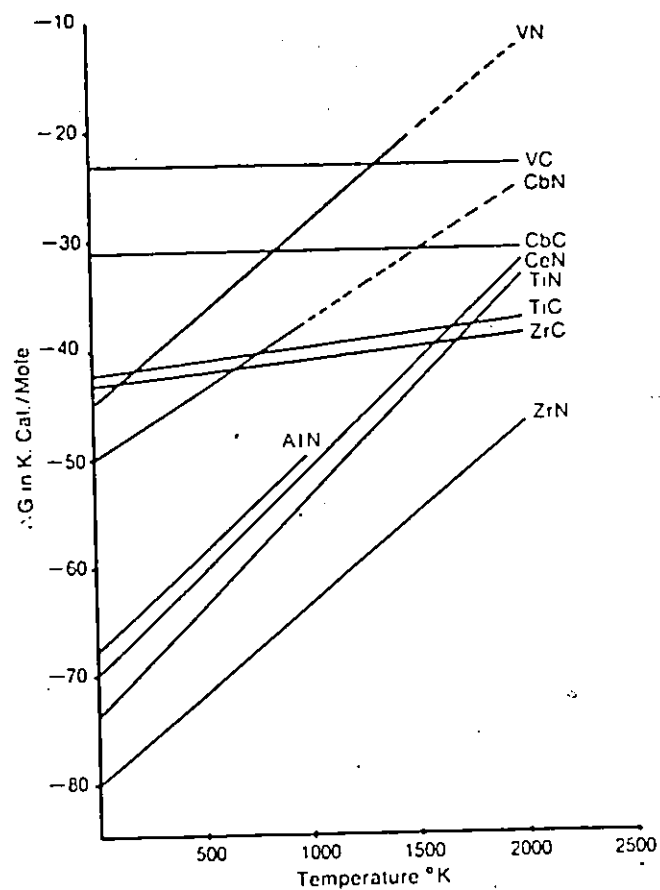


Figure 23 : Free Energy of Formation of Carbides and Nitrides. (Ref. 20)
 Note: Columbium (Cb) = Niobium (Nb).

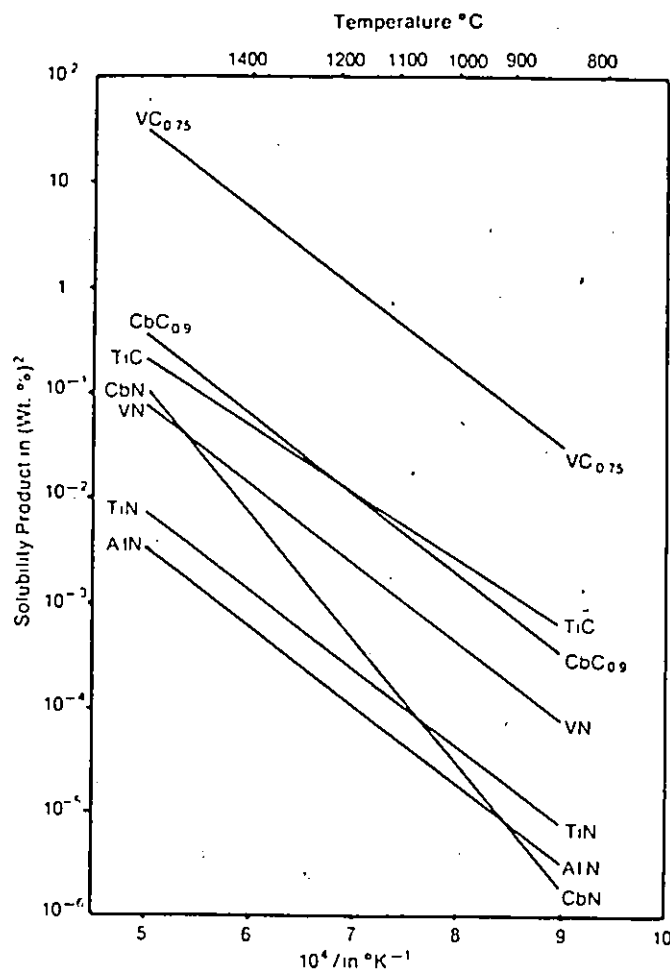


Figure 24 : Equilibrium Solubilities of Carbides and Nitrides in Austenite. (Ref. 20)
Note: Columbium (Cb) = Niobium (Nb).

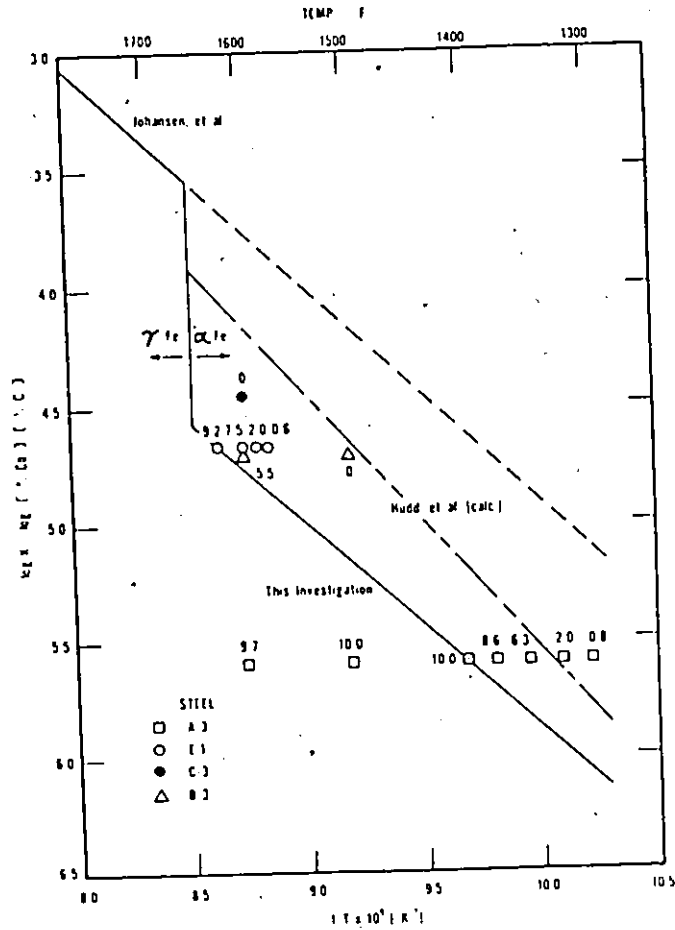


Figure 25 : The Solubility Product of CbC in Alpha-Iron Estimated From the Response of Yielding Behaviour to Annealing Temperature for Columbium-Treated Steels. (After Hook et al Ref. 12)

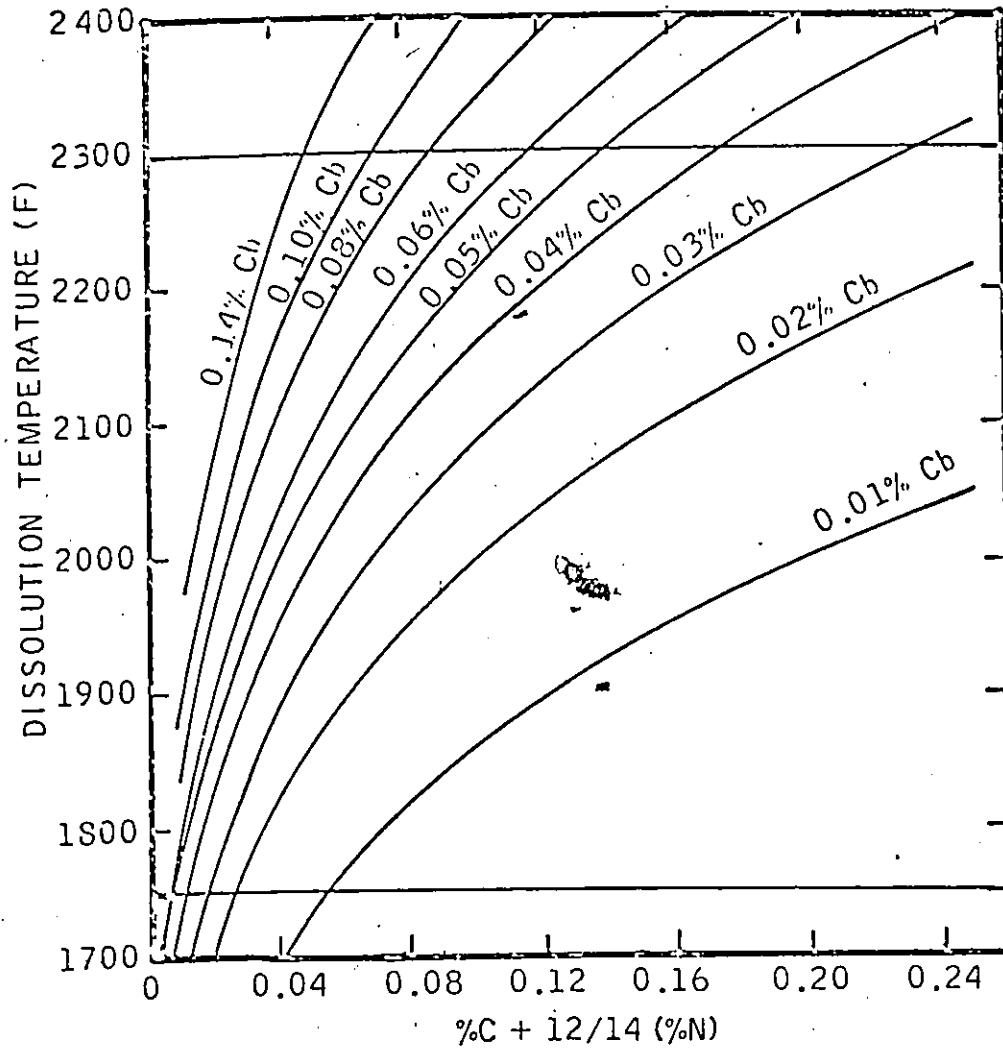


Figure 26 : Equilibrium Stability of Niobium (Columbium) Carbonitride in Austenite. (After Cryderman Ref. 14)

can be seen that for typical levels of elements used in steels, vanadium is less likely to precipitate in austenite, but will precipitate in ferrite. Niobium, on the other hand, can precipitate in the austenite and is thus useful for retarding austenite grain growth during deformation. Precipitates formed at the high temperatures would tend to be coarse and cannot provide much increase in strength, but precipitates formed in the ferrite at lower temperatures provide precipitation strengthening.

During welding, several effects may occur in the HAZ related to the precipitates. In the lower temperature regions, further precipitation may occur if this was not already complete and at the high temperatures some coarsening of the precipitates may occur. In the austenitic region, where the temperature is not sufficiently high to dissolve the precipitates, any coherency will be lost during the transformation. In the high temperature part of the HAZ the precipitates will dissolve. The fact that the grain size is the same in the coarse grain region of a fine grained steel as in a coarse grained steel, suggests that all precipitates dissolve in this region even in relatively low energy welds. Some recent work⁽³⁹⁾ has attempted to produce precipitates using titanium that are stable up to very high temperatures and essentially prevent the formation of a coarse grained region. The temperature at which dissolution will occur will depend on the quantity of each element

present and under equilibrium conditions may be estimated from the solubility data (Figure 24). Under the rapid thermal cycle of the HAZ the temperature is expected to be higher than in the equilibrium case.

Whether or not precipitates reappear on cooling is a question of kinetics. For precipitation to occur, supersaturation is required and sufficient temperature for diffusion processes. Precipitation is enhanced by deformation and gross deformation is absent from the HAZ. At cooling rates experienced in welds, it is doubtful whether significant precipitation occurs except perhaps at very slow cooling rates (for example, in electroslog welds). The HAZ in the as-welded condition is, therefore, supersaturated and precipitation may occur on subsequent heating. Indeed, vanadium and niobium steels do reveal precipitation hardening during stress relief heat treatments in the HAZ⁽⁴⁰⁾.

The precipitation of aluminium nitride is fairly sluggish and even in conventional rolling does not occur until below 800°C (see Figure 5). The lack of precipitation of nitrides in the coarse grain HAZ would mean that the free nitrogen could contribute to deterioration of toughness (Figure 27). Effective precipitation would occur during a subsequent heat treatment for stress relief.

The question of the significance of precipitation in the HAZ during welding is under debate. Some investigators claim that toughness deterioration is due to precipitation hardening (in niobium steels) but convincing evidence of the precipitates is lacking.

Heat treatment of the HAZ at a temperature of about 650°C may result in a number of metallurgical changes. Considerable changes in the dislocation substructure (recovery) may result and the lowering of the dislocation density may result in a drop of yield strength and an improvement in toughness. If low temperature transformation products, such as martensite, are present, tempering may occur with improvement in the toughness. As previously pointed out, the presence of microalloy elements in supersaturated solution can result in precipitation during subsequent heating. This, in the case of vanadium and niobium, could lead to an increase in yield strength and loss of toughness. Removal of free nitrogen may also occur and would be beneficial.

6. REVIEW OF TOUGHNESS STUDIES ON THE HAZ OF MICROALLOY STEELS

Several studies of the HAZ toughness have been conducted during the last decade. In an early study Aronson⁽⁴¹⁾ used simulated specimens to determine the effect of peak temperature on the strength and toughness in the HAZ of a steel with 0.065% C, 1.06% Mn and

0.041% Nb. Specimens with a peak temperature of 1060°C (1950°F) showed a drop in strength below that of the base material. In a real weld, where such a zone would be narrow, constraint effects would prevent the joint as a whole showing low strength. Regions heated to lower temperatures showed higher strength attributed to precipitation hardening. The impact transition temperature increased slightly in specimens heated to 730°C (1350°F) attributed to precipitation of NbC. Peak temperature of 850°C (1570°F) showed improved toughness (attributed to precipitate coarsening and fine grain size) and specimens heated to higher temperatures showed deterioration in toughness attributed mainly to grain coarsening (Figure 28).

An extensive study by Kaae and colleagues⁽⁴²⁾⁽⁴³⁾ at BWRA (Welding Institute) of a niobium bearing low carbon steel revealed evidence of HAZ softening only in very high heat input welds (electroslag) and this was a phenomenon not likely to cause problems in practice. The HAZ toughness of manual metal arc and submerged-arc welds was superior to that of the base material for both impact and static tests, except that static tests on manual welds showed a deterioration of toughness. Electroslag welds notched in the coarse grain region showed gross deterioration of toughness, the shift of transition temperature being attributed to coarse grain size and lowering of upper shelf energy to sulphide films. The steels used,

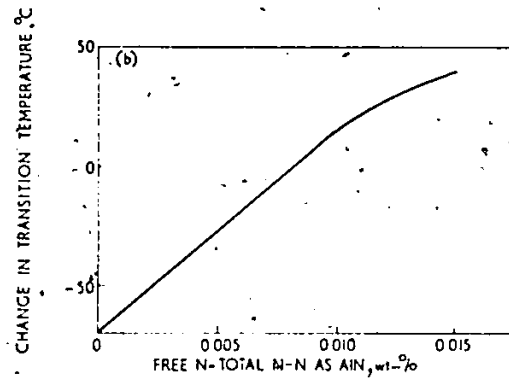


Figure 27 : Effect of Soluble Nitrogen on Impact Properties. (After Irvine Ref. 7)

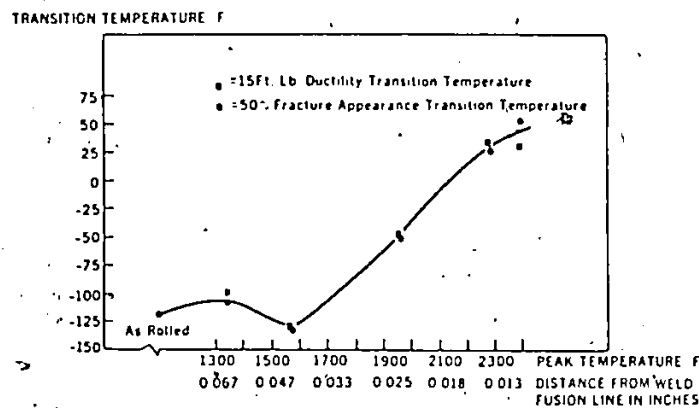


Figure 28 : Transition Temperature in °F vs. Peak Temperature in °F. Distance from Weld Fusion Line to Indicated Temperature is also Shown. (After Aronson Ref. 41)

by Kaae had 0.024% Nb, which is below levels currently popular in microalloy steels (Figure 29).

Dolby⁽⁴⁴⁾ made a comparison between real HAZ's and simulated specimens (Figure 30). He found the toughness essentially the same and concluded that simulation was a useful technique for studying HAZ toughness although yielding and load at fracture were different. This direct comparison is useful since several other workers have used simulation techniques. Saunders⁽⁴⁰⁾ studied the effect of post-weld heat treatment on the fracture toughness of C-Mn and low alloy steels, using COD techniques. Three of the steels showed a deterioration in the coarse grain HAZ. A semi-killed C-Mn steel (A) showed no deterioration, whereas a higher carbon fully killed C-Mn steel did (B), Figure 31. The former produced a pearlite/bainite structure in the HAZ, whereas the latter formed bainite/martensite, this latter structure having much lower toughness. Post-weld heat treatment improved the toughness of all the steels and appropriate choice of temperature could restore the original parent plate properties. A higher temperature was required for the vanadium containing steels. Saunders measured the HAZ hardness and when the post-weld heat treatment was expressed in terms of a Holloman-Jaffe parameter, a marked precipitation hardening effect at 550°C was noted in the steel containing 0.08% vanadium (Figure 32). Saunders concluded

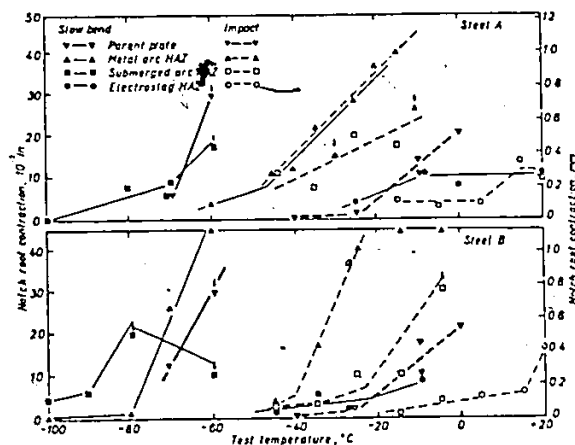


Figure 29 : Results of Fracture Toughness Tests on Niobium Treated, Low Carbon Manganese Steels. (After Kaae Ref. 43)

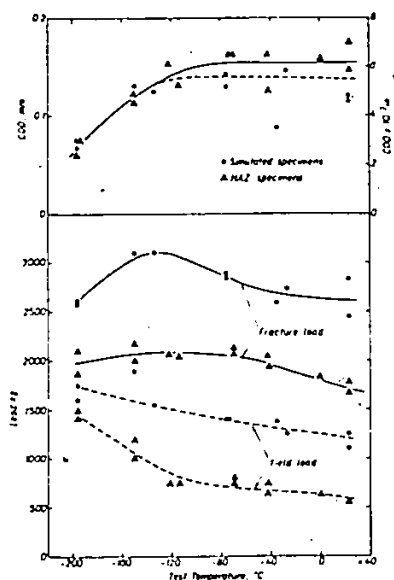


Figure 30 : Test Results for Simulated and Weld HAZ Specimens. Grain Coarsened Region. (After Dolby Ref. 44)

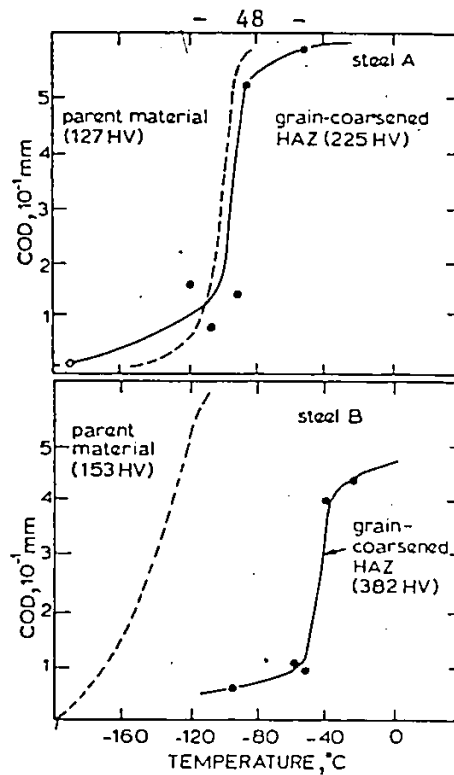


Figure 31 : COD Transition Curves for Parent Material and As-Welded Transformed Grain-Coarsened HAZ of a 1 kJ/mm Weld on Two C-Mn Steels. (After Saunders Ref. 40)

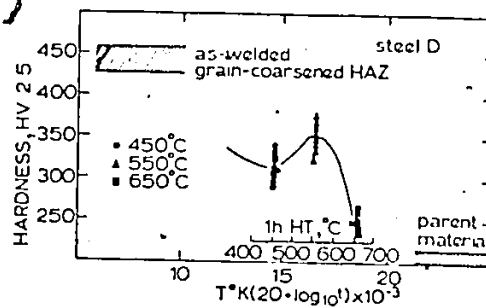


Figure 32 : Variation of HAZ Hardness in Steel Containing Vanadium with a Holloman-Jaffe Time/Temperature Parameter. (After Saunders Ref. 40)

that the best post-weld heat treatment to give optimum HAZ toughness was that which produced a fully over-aged condition.

Dolby and Saunders⁽⁴⁵⁾ reviewed several programs of testing at the Welding Institute and determined the metallurgical factors influencing the HAZ toughness. Almost all steels of the C-Mn or low alloy type showed embrittlement. In non-grain refined steels, maximum embrittlement occurred in the subcritical HAZ after welding over a notch. Dynamic strain ageing was thought to play an important role in this and in aluminium treated C-Mn steels this type of embrittlement was small. Depending on the composition of the C-Mn steels, martensite could be formed in the transformed HAZ and give embrittlement. In the coarse grained transformed region, the presence of grain refining elements, such as aluminium, was not significant. In other regions of the HAZ, grain refined steels showed better toughness than those not grain refined. Increasing energy input could improve toughness in the C-Mn steels if it reduced the amount of untempered martensite, but in low alloy steels increasing energy input generally caused a drop in toughness due to increased austenitic grain size and increased amount of bainite.

The subcritical HAZ has received a lot of attention at the Welding Institute because welding over a defect, whose tip coincides with

the subcritical location in the HAZ, is a situation that arises in the Well's wide plate test. Dolby and Saunders⁽⁴⁶⁾ found that embrittlement was most severe for semi-killed steels, but less so for those containing aluminium. Removal of nitrogen from interstitial solution reduced the dynamic strain ageing capacity of the steel.

The toughness of the HAZ of submerged-arc welds in C-Mn steels containing Al or Nb or both was studied by Cane and Dolby⁽⁴⁷⁾, using COD techniques. Marked embrittlement in the HAZ was noted in the grain refined steels when welded with 5 and 7 kJ/mm. Less embrittlement was noted in a plain C-Mn steel. The lowest HAZ toughness was recorded in the niobium containing steels, although the parent materials had similar toughness. The authors explained the effect of niobium in terms of its effect on the microstructure. Proeutectoid ferrite was suppressed and transformation to upper bainite was promoted. The magnitude of the embrittlement is seen in their results for the coarse grain region of a C-Mn-Nb steel (Figure 33).

Dolby and Knott⁽⁴⁸⁾ made a detailed study of martensite structures typical of those that could form in the HAZ of low alloy steels. When fracture initiated by quasi-cleavage in martensite structures, the toughness depended on the prior austenite grain size (Figure

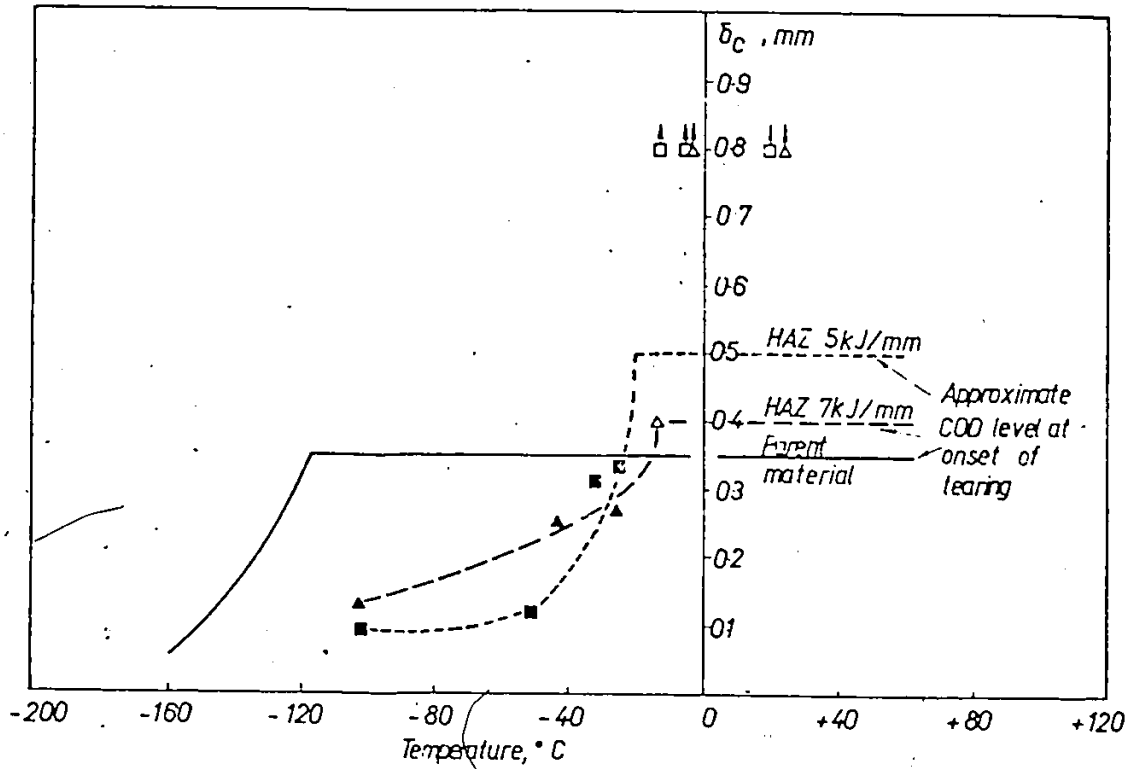


Figure 33 : Transition Curves From Grain Coarsened HAZ's; C-Mn 0.056% Nb Steel. (After Cane et al Ref. 47)

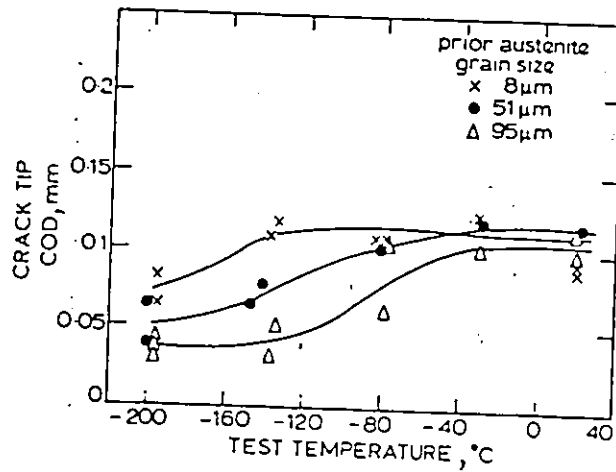


Figure 34 : Fracture Toughness of Martensitic Structures of Varying Prior Austenite Grain Size; Specimen Size 10 mm Square Section x55 mm. (After Dolby and Knott Ref. 48)

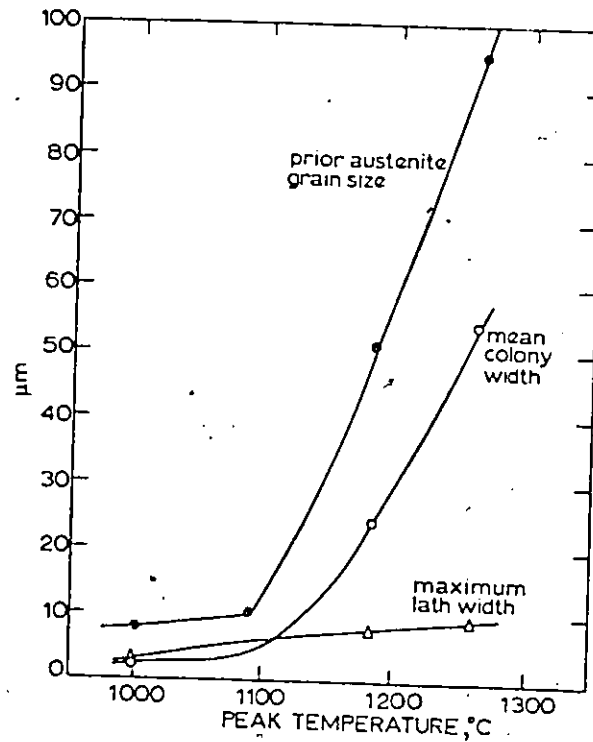


Figure 35 : Variation of Prior Austenite Grain Size, Martensite Lath Width and Colony Width with Peak Temperature During Heat Treatment. (After Dolby and Knott Ref. 48)

34), the controlling factor being the martensite colony width (Figure 35). Toughness was lowered when upper bainite was introduced into the structure. When fracture initiated by microvoid coalescence, it was less dependent on prior austenite grain size and depended mainly on inclusion and carbide population.

The growing use of microalloy elements, such as niobium and vanadium, has prompted studies of the effects of these elements on the HAZ toughness. As the foregoing summary indicates, there is evidence of a detrimental effect of niobium, particularly at high energy inputs. Hannerz⁽⁴⁹⁾ made a particular study of the effect of niobium on the HAZ toughness, using simulated specimens, his specimens representing the coarse grain region of high and low energy input welds. He showed an increase in transition temperature with increasing niobium content for both cases (Figure 36). This trend was also observed in a low carbon (0.03%) steel. As expected, the deterioration was worse for the slower cooling rates. Hannerz attributed the loss of ductility to precipitation hardening, although there was not clear evidence of precipitation. The same group⁽⁵⁰⁾ also studied the effect of vanadium and showed a deterioration of HAZ properties (in simulated specimens) for high energy welds when the vanadium exceeded about 0.10%. Low energy welds were tolerant to levels of vanadium up to 0.20% without any deterioration. Some evidence suggests that low levels of vanadium, particularly with low carbon, may be beneficial⁽⁵²⁾ (Figure 37).

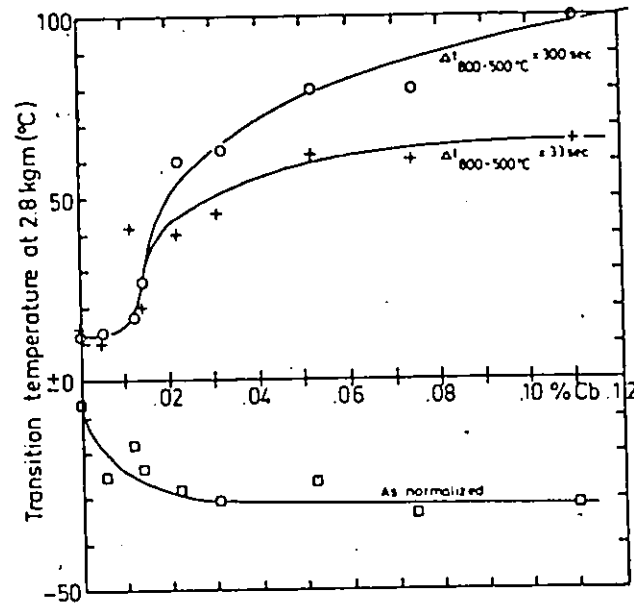


Figure 36 : Transition Temperature for a C-Mn Steel in Normalized and in As-Welded Simulated Condition Showing Effect of Niobium Content. (After Hannerz Ref. 49)

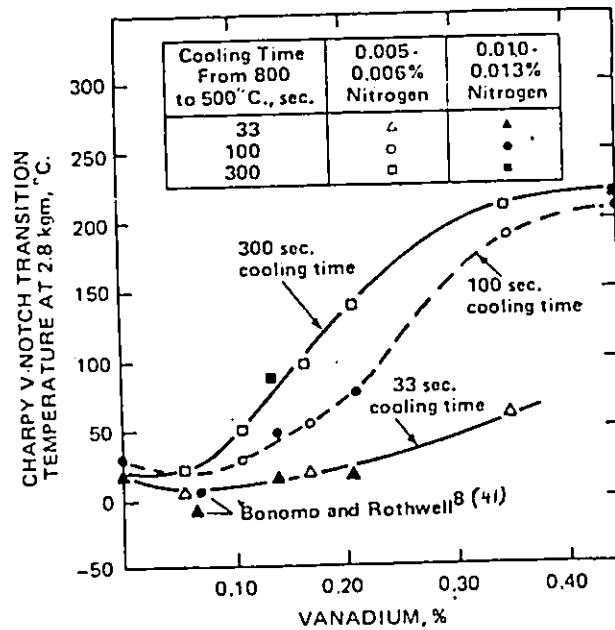


Figure 37 : Influence of Vanadium on the Simulated Heat-Affected-Zone Transition Temperature after Hannerz and Jonsson-Holmquist. (After Hart Ref. 51. Data From Ref. 50 & 52)

The popularity of niobium and other microalloys in steels for pipelines has stimulated studies of HAZ toughness in high energy submerged-arc welds typical of those used for the longitudinal seams of welded pipes. Wada⁽⁵³⁾ made tests on the HAZ of welds in Mn-Mo-Nb steels, using a multipass weld that produced a planar HAZ. Charpy impact tests were used and in such a weld the total energy recorded would result from crack propagation through a range of microstructures. He found the lowest region of toughness to be in the coarse grain region and also found a region of slight drop in toughness just outside the visible HAZ. Increasing niobium or energy input lowered the toughness in the coarse grain region, although the results shown in Figure 38 do not have a constant base chemistry. With control of these two factors, he was able to obtain sufficient toughness to meet the requirements of the particular application. Sawhill⁽⁵⁴⁾⁽⁵⁵⁾⁽⁵⁶⁾ took CVN specimens from two-pass welds representing typical pipeline welds. These specimens include part weld metal, part HAZ and part parent plate, and his results show the influence of the prior treatment of the steel (Figure 39). Results from this test were better than from the planar HAZ tests because of the geometry of the weld. Sawhill and Wada⁽⁵⁷⁾ found precipitation hardening by Nb (C,N) to be significant in the coarse grain region when reheated by subsequent passes. This increased with increasing niobium content.

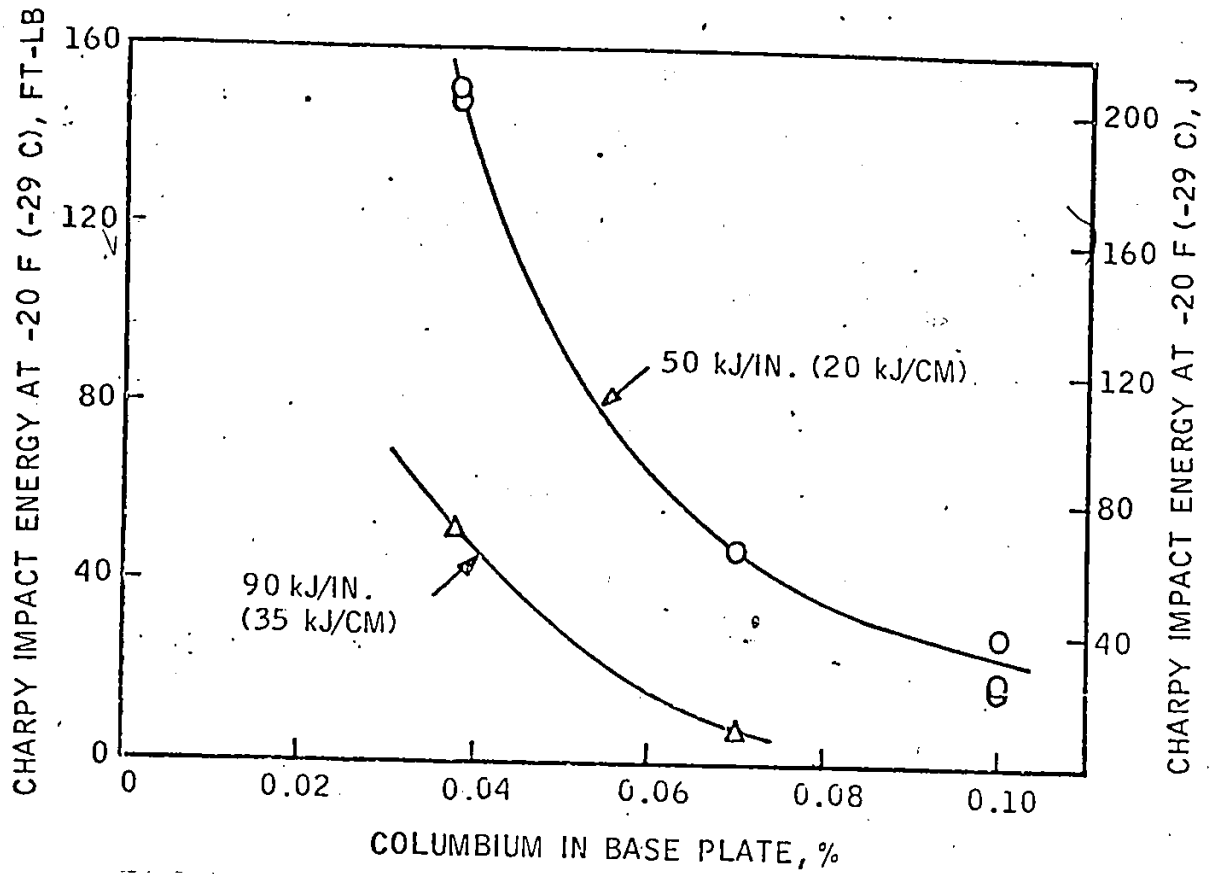


Figure 38 : Charpy Impact Toughness of Fusion Line at -20°F (-29°C),
Plotted Against Columbium Content of Base Plates.
(After Wada Ref. 53)

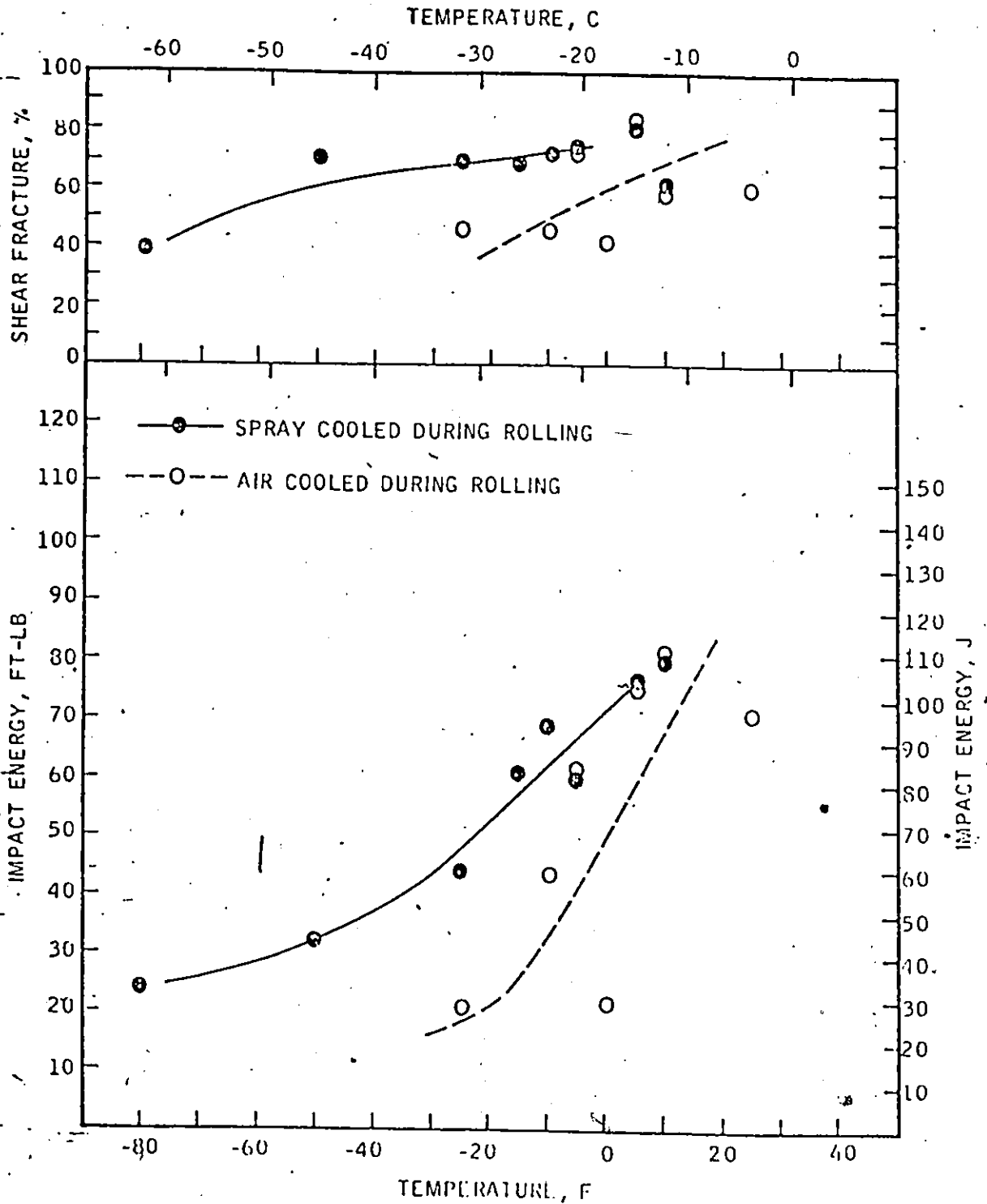


Figure 39 : Impact Transition Curves for Full Size Charpy Impact Specimens Notched in the "50/50" Position of Mo-Cb Steel Welds. (After Sawhill Ref. 55)

These general effects of energy input and microalloy content have been observed by several other investigators⁽⁵⁸⁻⁶¹⁾. In many cases the deterioration of toughness in the HAZ is not so serious as to present a fracture risk in the intended application, but the trends indicate that potential fracture problems related to HAZ toughness must be considered in future steel design and further applications of the steels.

The effects of various alloying elements was studied by Ito et al⁽⁶²⁾. None of their steels has niobium, but vanadium up to 0.1% was present in some. They found they could relate the CVN transition temperature of the bond region (coarse grain HAZ close to the fusion boundary) to the composition with a linear model. The formula depended on whether martensites and lower bainites were formed or whether ferritic and upper bainitic structures were formed (Figures 40 and 41). In the latter case, only nickel and molybdenum were beneficial. It is worth noting that vanadium up to 0.1% was not significant. Carbon was the most detrimental and this is emphasized by Miyoshi et al⁽⁶³⁾, who used the COD test for assessing the HAZ (Figure 42). They found that prior history of the steel does not influence toughness in the coarse grain region but may be significant away from the fusion boundary. Energy input and its effect on cooling time and grain size were important. At low energies the toughness was independent of cooling rate. Toughness

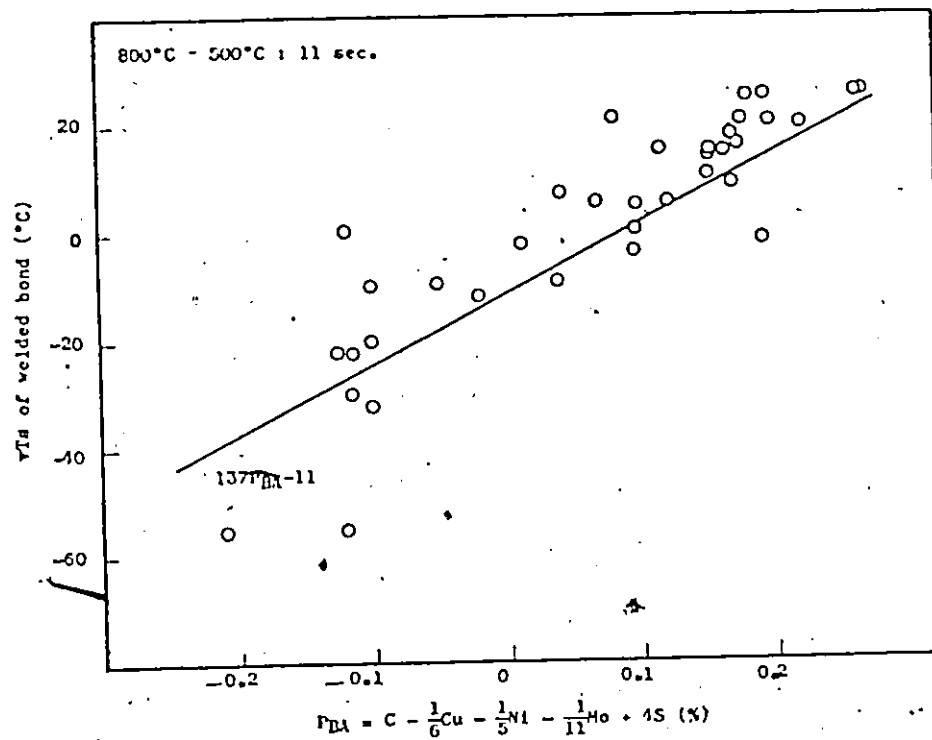


Figure 40 : Relationship Between Formula of Susceptibility in Steel for Bond Brittleness (P_{BA}) and Measured Charpy Transition Temperature vT_s of Welded Bond When Quenched Microstructure of Martensites and Lower Bainite were Formed in the Cooling Time on the Critical Range of About 11 sec. (After Ito et al Ref. 62)

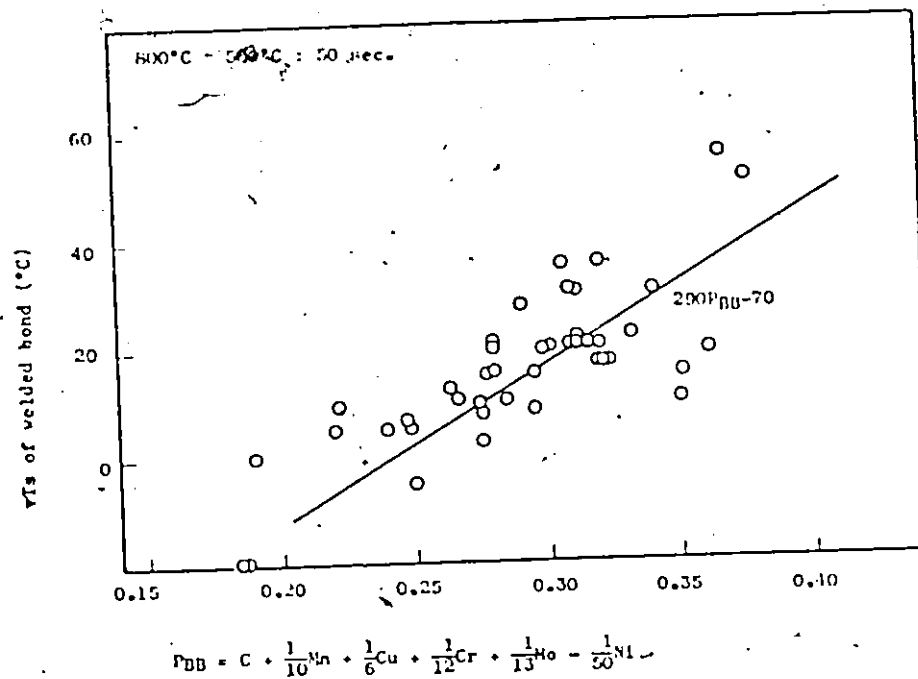


Figure 41 : Relationship Between Formula of Susceptibility in Steel for Bond Brittleness (P_{BB}) and Measured Charpy Transition Temperature vTs of Welded Bond When the Intermediate Microstructure of Upper Bainites and Ferrites were Formed in the Cooling Time on the Critical Range of About 50 sec. (After Ito et al Ref. 62)

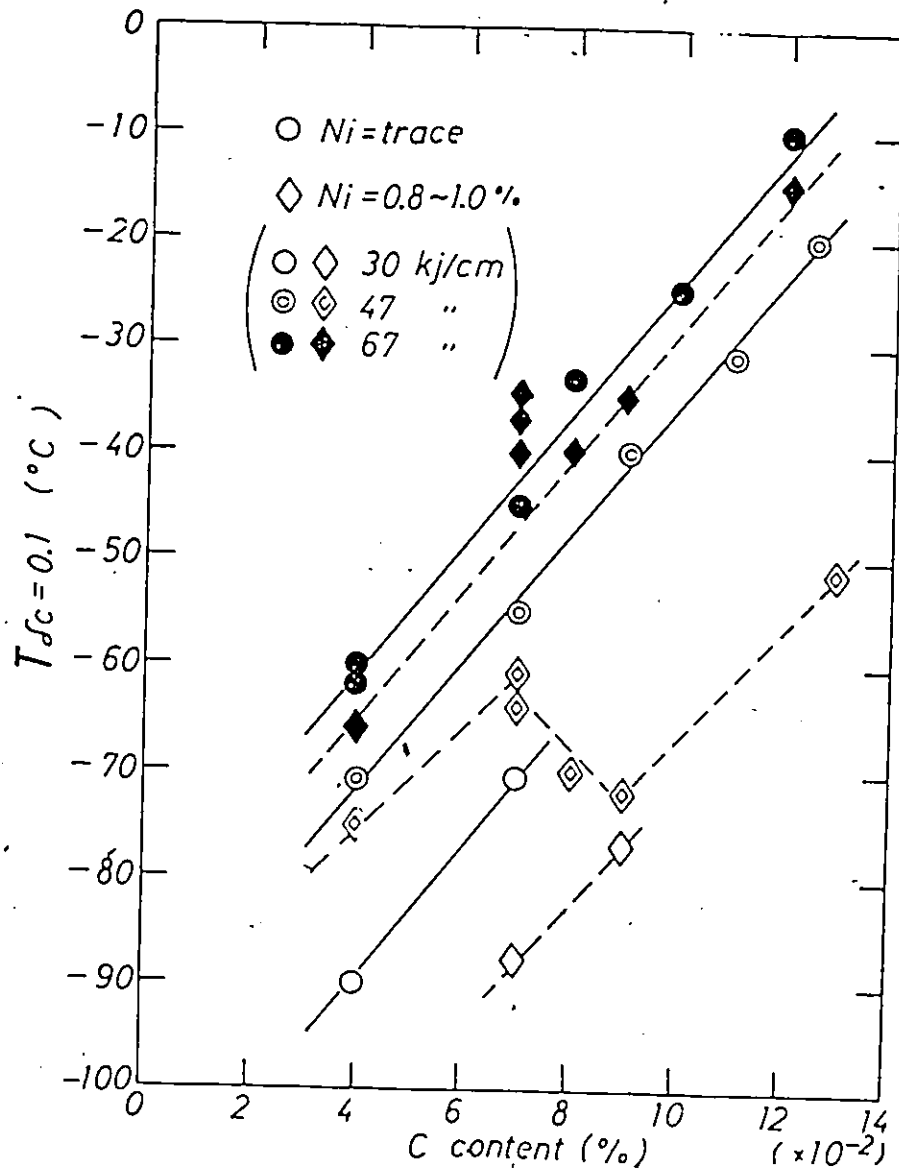


Figure 42 : The Relation Between $T_{Sc} = 0.1$ and C Content. The Vertical Axis is the Transition Temperature for a Critical Crack Opening Displacement (COD) of 0.1 mm and Represents the Toughness in Slow Loading Conditions. (After Miyoshi et al Ref. 63)

could be improved by promoting low carbon martensite by low energy welds (MIG), or alloying with Mn, Mo or Ni.

Effects of alloying elements were studied by Shiga et al⁽⁶⁴⁾ using simulation techniques. The subcritical and coarse grained regions showed deterioration of toughness in the microalloyed steels (Figure 43). They found a harmful effect of vanadium when molybdenum was present, which was attributed to an increase in the amount of vanadium in solution. This is a view contrary to opinions held by others who feel that precipitation is likely to do more harm.

Recent data on the toughness of the HAZ of niobium steels has been published by Graville and Rothwell⁽⁶⁵⁾. They used an instrumented Charpy test with specimens containing fatigue cracked notches. This technique avoided the uncertainties of simulation techniques, but also enabled the crack initiation toughness at the point of interest in the HAZ to be studied. Experimental steels with various levels of niobium were used and a range of cooling rates was covered. The results showed that cooling rate had a far larger effect than the niobium level. At slow cooling rates, the toughness decreased with increasing niobium content and at fast cooling rates small levels of niobium were beneficial to the toughness. Results are shown in Figure 44.

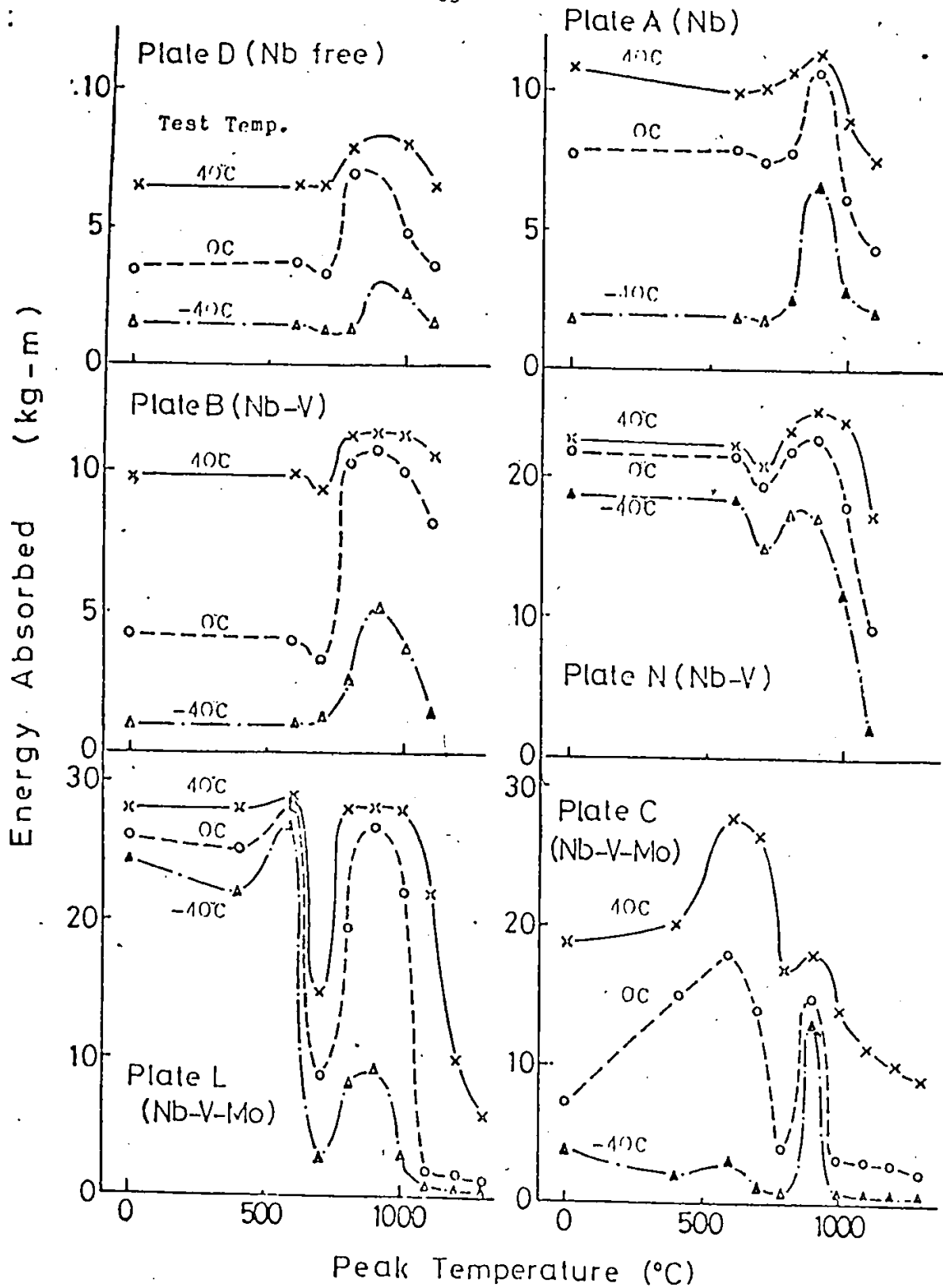


Figure 43 : Toughness of Synthetic Weld Heat-Affected-Zone. The Parent Material Properties Have Been Changed by the Rolling Schedule. (After Shiga et al Ref. 64)

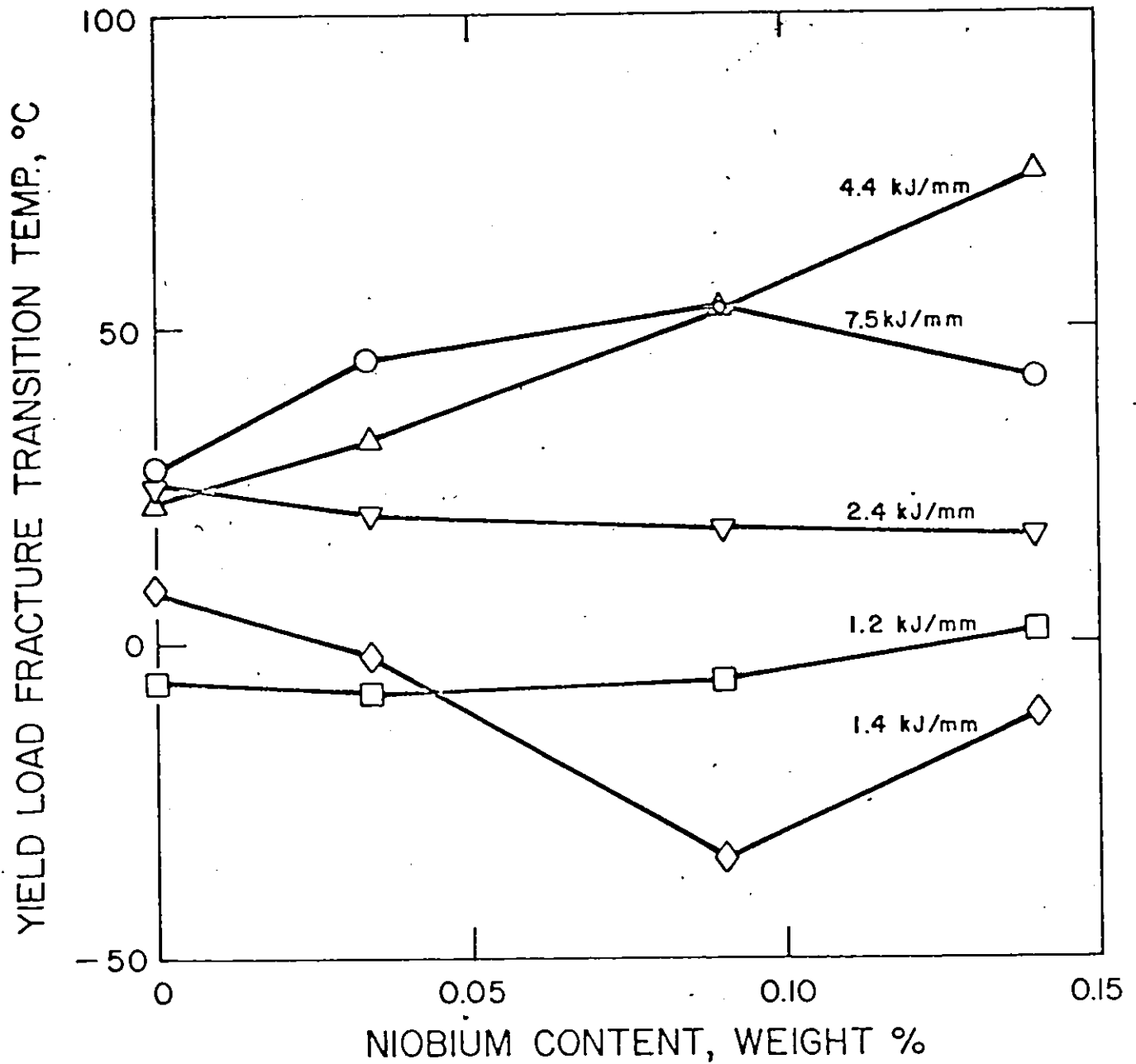


Figure 44 : Variation of Yield Load Fracture Transition Temperature with Niobium Content for Four Heat Inputs: Lowest Heat Input is on 25 mm Plate. Cooling Times From 800-500°C Shown in Brackets. (Ref. 65)

In some recent interesting developments attempts have been made to restrict grain growth in the HAZ. Achieving this by limiting energy input of the weld is often unattractive economically, since this limits the volume of weld metal added in a given time. The advantages in many cases of using high energy has prompted the development of steels that would resist grain growth. Some success⁽³⁹⁾ has been obtained using titanium nitride precipitates of a suitable size. Titanium nitride could resist grain growth up to 1400°C. Experimental steels containing about 0.02% Ti were found to resist grain growth and the resulting microstructure in the HAZ gave improved toughness. The beneficial effects of titanium have been confirmed elsewhere⁽⁶⁶⁾⁽⁶⁷⁾, but the developments are relatively new and the steels are not commercially available.

Although some of the results given in the preceding section may appear contradictory at first sight, most can be rationalized when the precise welding conditions and steel composition are taken into consideration. Decrease in toughness is noted when high energy welds are made which lead to grain coarsening in the heat-affected-zone. Detrimental effects of niobium can occur at high energy, probably because of precipitation of carbo-nitrides. A more severe decrease in toughness occurs on stress relief, presumably because of more complete precipitation. At low energy inputs niobium can have a beneficial effect in the lower carbon steels probably because

of its effect in reducing the amount of proeutectoid grain boundary Ferrite. Recent work shows that the influence of composition is far less than that of cooling rate. This means that in any fine grained steel with good toughness the heat input to the weld may have to be limited in order to retain adequate properties. The recent developments on titanium steels, however, show that grain growth in welding may be resisted by titanium nitrides of carefully controlled size. Such steels would allow high heat input processes to be used without detrimental effects on properties.

7. SUMMARY AND CONCLUSIONS

Weldability is essential to any modern steel for structural purposes and its meaning takes on more than simply resistance to cracking. Because of the composition of modern steels, the reliance on grain refinement and the complex processing they receive, the effect of the heat of welding becomes of vital importance. Deterioration of properties in the heat-affected-zone could limit the application of the material or severely limit the use of welding.

In this report the physical metallurgy of the heat-affected-zone has been reviewed with particular emphasis on the fracture toughness of the HAZ in microalloyed steels. The following conclusions are drawn from this review:

- (a) Classical heat flow theory using equations based on point source theory, but with empirically determined constants, can quite accurately predict cooling rates and temperature distributions some distance from the weld. The theory is not adequate close to the weld, or at high temperatures where the exact distribution of the heat in the source becomes important.
- (b) Grain growth of the austenite in the region close to the fusion boundary is controlled mainly by the temperature gradient, except in titanium nitride steels, where precipitates may not dissolve. No adequate model for grain growth exists and this would be a very useful area for further work.
- (c) The effect of composition and cooling rate on HAZ toughness is complex and can only be predicted in a general sense. High energy welds would be expected to cause a deterioration due to grain growth. Niobium may precipitate in a high energy slowly cooled weld and cause further deterioration. Vanadium does not have a significant effect.
- (d) Niobium may have a beneficial effect at low energy input due to reduction in the amount of proeutectoid grain boundary ferrite.
- (e) In the stress-relieved condition improvements in toughness may occur in some steels, such as those containing aluminium, due

to the removal of free nitrogen from solution. Stress relieving may have an adverse effect in some steels, such as those containing high levels of vanadium or niobium due to precipitation hardening.

- (f) The use of titanium nitride to resist grain growth appears to be a promising solution to the problem of high energy welds.

REFERENCES

1. Morrison, W.B. and Woodhead, J.H., Journal of Iron and Steel Institute, 201 Page 43 (January) 1963.
2. Morrison, W.B., Ibid Page 317 (April).
3. Irvine, K.J., and Pickering, F.B., Journal of Iron and Steel Institute, 201 Page 944 (November) 1963.
4. Gray, J.M., Webster, D., and Woodhead, J.H., Journal of Iron and Steel Institute, 203 Page 812 (August) 1965.
5. Webster, D., and Woodhead, J.H., Journal of Iron and Steel Institute, 202 Page 987 (December) 1964.
6. Irvine, K.J., Pickering, F.B., and Gladman, T., Journal of Iron and Steel Institute, 205 Page 161 (February) 1967.
7. Duckworth, W.E., Phillips, R., and Chapman, J.A., Journal of Iron and Steel Institute, 203 Page 1108 (November) 1965.
8. Duckworth, W.E., and Baird, J.D., Journal of Iron and Steel Institute, 207 Page 854 (June) 1969.
9. Vanderbeck, R.W., Welding Journal Research Supplement (March) 1958 Page 114-115.
10. Irvine, K.J., Gladman, T., Orr, J., and Pickering, F.B., Journal of Iron and Steel Institute, 208 Page 717 (August) 1970.
11. Gray, J.M., Met. Trans. 3 Page 1495 (June) 1972.
12. Hook, R.E., and Elias, J.A., Met. Trans. 3 Page 2171 (August) 1972.
13. Gray, J.M., and Wilson, W.G., 14th Mechanical Working and Steel Processing Conference, Chicago, January 19, 1972.
14. Cryderman, R.L., Coldren, A.P., Smith, Y.E., and Mihelich, J., Mechanical Working and Steel Processing Proceedings, AIME Vol. X, 1972.
15. Gray, J.M., "Metallurgy of High-Strength Low Alloy Pipeline Steels: Present and Future Possibilities" Dallas, Texas, January 18, 1972.

16. Gray, J.M., Int. J. Pressure Vessels and Piping 2 Page 95 (1974).
17. Wilson, W.G., Metals Engineering Quarterly Page 1 (May) 1974.
18. Nakamura, H., and Kuriyama, Y., Ishikawajima-Harima Heavy Industries Co. Ltd. April 1963.
19. Pickering, F.B., Microalloying '75 Washington October 1, 1975.
20. Koul, M.K., Metals Engineering Quarterly 16 (1) Page 1 February 1976.
21. Paley, Z., and Hibbert, P.D., Welding Journal 54 Research Supplement Pages 385-s to 392-s (November) 1975.
22. Graville, B.A., "The Principles of Cold Cracking Control in Welds" Dominion Bridge Company Ltd., Montreal 1975.
23. Graville, B.A., Welding Journal 52 (9) Res. Suppl. Pages 377-s to 385-s (September) 1973.
24. Myers, P.S., Uyehara, O.A., and Borman, G.L., WRC Bulletin No.123 (July) 1967.
25. Maynier, P.H., Martin, P.F., and Bastien, P., Memoires Scientifiques de la Revue de Metallurgie (mars) 1967.
26. Schmidtman, E., and Rippel, M., Schweissen und Schneiden 27 (7) Pages 261-265 1975.
27. Ikawa, H., Shin, S., and Oshige, M., Trans. Japan Welding Society 4 (2) Pages 35-41 (September) 1973.
28. Hopkin, G.L., Welding Journal 23 (11) Res. Suppl. Pages 606-s to 608-s.
29. Doan, G.E., Stout, R.D., and Frye, J.M., Welding Journal 22 (7) Res. Suppl. Pages 278-s to 299-s (July) 1943.
30. Watkinson, F., and Baker, R.G., Brit. Weld. Journal 14 (11) Pages. 603-613 (November) 1967.
31. Rose, A., Atlas of CCT Curves, Max Planck Institute, Dusseldorf.
32. Granjon, H., and Gaillard, R., Memoires Scientifiques Rer Met LXIV No. 4 Pages 335-343 1967.

33. Graville, B.A., and Read, J.A., Welding Journal 39 (4) Res. Suppl. Pages 161-s to 169-s (April) 1974.
34. Graville, B.A., Paper Presented at Conference on Welding of HSLA Steels, Rome, Italy, 9 November 1976. To be Published by ASM.
35. Cottrell, C.L.M., Jackson, M.D., and Whitman, J.G., Welding Res. 5 (8) Pages 201-215 (August) 1951.
36. Bailey, N., "Welding Procedures for Low Alloy Steels" Welding Institute Report (July) 1970.
37. Coe, F.R., "Welding Steels Without Hydrogen Cracking" Welding Institute 1973.
38. Grossman, M.A., Trans. AIME 150 Page 227 1942.
39. Ikeno, T., Kanazaura, S., Nakashima, A., and Okamoto, K., Tetsu to Hagare 59 (4) Page S148, 1973.
40. Saunders, G.G., "Influence of Welding and Post-Weld Heat Treatment on the HAZ Fracture Toughness of C-Mn and Low Alloy Steels" Iron and Steel Institute Biennial Conference on Heat Treatment, 8-9 December 1971.
41. Aronson, A.H., Welding Journal 45 Research Supplement Pages 266-s to 271-s (June) 1966.
42. Kaae, J.L., British Welding Journal 15 (8) Pages 395-407 (August) 1968.
43. Kaae, J.L. and Bailey, N., Metal Construction and British Welding Journal 1 (8) Pages 371-377 (August) 1969.
44. Dolby, R.E., Metal Construction 4 (2) Pages 59-63 (February) 1972.
45. Dolby, R.E. and Saunders, G.G., "Metallurgical Factors Controlling the HAZ Fracture Toughness of Carbon-Manganese and Low Alloy Steels" Welding Institute March 1974.
46. Dolby, R.E. and Saunders, G.G., Metal Construction 4 (5) Pages 185-190 (May) 1972.
47. Cane, M.W.F. and Dolby, R.E., Welding Research International 4 (3) Pages 51-72 1974.
48. Dolby, R.E. and Knott, J.F., Journal of Iron and Steel Institute 210 Pages 857-866 (November) 1972.

49. Hannerz, N.E., Welding Journal 54 (5) Research Supplement Pages 162-s to 168-s (May) 1975.
50. Hannerz, N.E., and Jonsson-Holmquist, B.M., Metal Science Journal 8 (7) Page 228, 1974.
51. Hart, P.H.M., Dolby, R.E., Bailey, N. and Widgery, D.J., "The Weldability of Microalloyed Steels" Micro Alloying '75, October 2, Washington, 1975.
52. Bonomo, F. and Rothwell, A.B., Proceedings of the International Welding Congress, Bratislava, Pages 45-53, 1971.
53. Wada, T., Climax Molybdenum Report L-176 - 108 (March) 1974.
54. Sawhill, J.M., Climax Report ISJ-786 (August) 1973.
55. Sawhill, J.M., Climax Report J-4050 (March) 1974.
56. Sawhill, J.M., Climax Report L-176 - 123 (May) 1975.
57. Sawhill, J.M. and Wada, T., Welding Journal 54 (1) Research Supplement Pages 1-s to 11-s (January) 1975.
58. Matsushita, K., Nishiyama, N. and Tsuboi, J., IIW Doc. IX-879-74.
59. Banks, E.E., Australian Welding Journal, Pages 59-67 (Sept.-Oct.) 1974.
60. Banks, E.E., BHP Research Laboratories Report MRL/101/75/001 (March) 1975.
61. Banks, E.E., Welding Journal 53 (7) Research Supplement Pages 299-s to 306-s (July) 1974.
62. Ito, Y., Ikeda, M., Nakanishi, M. and Kohyama, A., IIW Doc. IX-842-73.
63. Miyoshi, E., Hasebe, S., Benyo, K. and Yamaguchi, Y., IIW Doc. IX-878-74.
64. Shiga, A., Imura, M. and Tsuboi, J., IIW Doc. IX-880-74.
65. Graville, B.A. and Rothwell, A.B., Metal Const. 9 (10) Pages 455-456 (October) 1977.
66. Granges Oxelosunds Jarnverk, Unpublished.

67. Sawhill, J.M. Boussel, P. and Morrow, J.W., Paper Presented at Conference on Weldability of HSLA Steels, Rome, Italy, November 9-12, 1976, to be Published by ASM.
-

NOTATION

The following notation has been used in the text where not otherwise defined:

T or Θ	-	temperature
T_0	-	initial plate temperature
\dot{Q}	-	rate of heat input
k	-	thermal conductivity
ρ	-	density
C	-	specific heat
λ	-	$= \rho C / 2k$
V	-	velocity (welding speed)
t	-	time
ξ	-	$= x - vt$ (moving coordinates)
r^2	-	$= \xi^2 + y^2 + z^2$
K_0	-	modified Bessel function of the second kind and zero order
δ	-	plate thickness
E	-	weld energy input